Report LR-641

Crack Opening Stress Measurements of Surface Cracks in 7075-T6 Al Alloy Plate Specimens through Electron Fractography

August 1990

Ichsan S. Putra and J. Schijve

TU Delft

Faculty of Aerospace Engineering

Delft University of Technology

Crack Opening Stress Measurements of Surface Cracks in 7075-T6 Al Alloy Plate Specimens through Electron Fractography

Ichsan S. Putra and J. Schijve

Table of Contents

SUMMARY

Crack opening stress measurements were carried out on 9.6 mm thick specimens of 7075-T6 Aluminium alloy with semi-elliptical surface cracks. Measurements were made through a fractographic technique based on a load sequence which can produce distinct striation characteristics on the fracture surface. The crack opening stress S_{op} is deduced from the striation pattern. The variation of S_{op} along the crack periphery and during crack extension was measured. Close to the front surface S_{op} is higher due to plane stress condition. At a large crack depth a strong influence of plasticity in the ligament on S_{op} was found, i.e. S_{op} decreases as the crack extends to breakthrough. The agreement of $da/dN = \Delta K_{eff}$ curves between surface cracks and through cracks data was only found for a limited range of crack depth of the elliptical cracks.

List of Symbols

a	= crack depth
c	= crack length on the surface
a/c	= aspect ratio of surface crack
a/t	= relative crack depth
K	= stress intensity factor
R	= stress ratio of fatigue load
r_p	= plastic zone size
S_{op}	= crack opening stress level (MPa)
S_{max}	= maximum stress (MPa)
S_{min}	= minimum stress (MPa)
S_{min}^*	= minimum stress in the S_{op} measuring block
$S_{0.2}$	= yield stress (MPa)
t	= thickness of the specimen
ΔK_{eff}	= effective stress intensity range
ΔS	= stress range
ΔS_{eff}	= effective stres range
ΔS_{min}^*	= difference of subsequent minimum stress in the S_{op} measuring block

1 INTRODUCTION

Since Elber introduced the crack closure concept [1] much attention has been paid to this phenomenon. Prediction models for crack growth under variable amplitude (VA) loading e.g. CORPUS, ONERA and PREFFAS were based on this concept. In order to apply the crack closure concept in prediction models accurate information on the crack closure level S_{op} is required. A survey of various techniques to measure S_{op} is given in [2]. The techniques can be classified into three main groups:

1. Direct observations of crack closure at the crack tip, employing a variety of means: the optical or scanning electron microscope, replica techniques, interferometry, interior displacement and transparent material.

2. Mechanical compliance measurement using a clip gage or a strain gage, and physical compliance measurements with a potential drop technique, eddy currents or ultrasonics.

3. Indirect methods based on crack growth measurements as affected by crack closure, which includes zero crack growth observation during variable amplitude loading, striation spacing measurements during variable amplitude loading, and calibration in a high stress ratio test.

Although these techniques confirm the occurrence of crack closure, discrepancies between published experimental results imply difficulties to achieve accurate and unambiguous crack closure stress levels. The difficulties arise from the fact that crack closure is a complex phenomenon which includes many aspects.

One aspect may be mentioned here, i.e the difference between plane strain and plane stress conditions at the crack tip. The difference of the state of stress along the crack front implies different sizes of the plastic zone. As a first approximation the size of the plastic zone can be estimated with:

$$r_p = \frac{1}{\pi\alpha}\left(\frac{K}{S_{0.2}}\right)^2$$

The factor α is usually taken to be 3 for plane strain and 1 for plane stress. This difference in plastic zone size leads to a higher closure level near to the specimen surface, which is in the plane stress condition. This surface phenomenon was demonstrated by Ewalds and Furnee [3], Fleck and Smith [4], Shaw and Le May [5] and some other investigators. For a growing fatigue crack it implies that the effective stress intensity factor near to the specimen surface is lower than at mid thickness. As a consequence the crack front on the surface will trail behind. The occurrence of trailing behind at the surface is usually found for part-through cracks.

Part-through cracks offer problems due to the variation of the stress intensity factor along the crack

periphery, and the variation of the local S_{op} resulting from different plastic zone sizes. In view of the influence of different closure levels on fatigue crack growth it is desirable to measure S_{op} locally along the crack front. For this purpose two different techniques are employed i.e. a fractographic technique with the electron microscope (SEM or TEM) and observations on transparent material.

The present paper addresses the fractographic technique to measure S_{op} of semi-elliptical cracks in 7075-T6 Aluminium alloy plate specimens. The crack growth rate of semi-elliptical cracks is related to the effective stress intensity factor calculated from the measured S_{op}. By adopting ΔK_{eff} it is expected that, the effect of the difference in constraint along the crack front is eliminated, which leaves the local ΔK_{eff} as the main parameter to describe the fatigue crack growth rate. Since similar ΔK_{eff} values will result in the same crack growth rate (similarity approach), it can be expected that the crack growth rate at different points along the crack front will fall in the same scatter band as obtained for through cracks.

In the present investigation fractographic S_{op} measurements were made for different initial notch geometries and different stress levels. To shed some more light on the fractographic technique to measure S_{op} a review of this method is given in the following section. Experimental procedures and results are presented in section three and four respectively. In section five the results are discussed, followed by a summary of the conclusions in section 6.

2 FRACTOGRAPHIC TECHNIQUE TO MEASURE S_{op}

The fractographic method to determine S_{op} is based on observations of the striation spacing. A striation is the trace of crack extension during an individual cycle, which is a function of ΔK_{eff}. It thus can provide an indication of S_{op}. In order to produce striations that can give indications of S_{op}, a characteristic load sequence should be applied. For part-through cracks this technique is qualitatively superior to the others because it can provide information on the variation of S_{op} along the crack periphery.

Pelloux et al. [6] carried out tests on a compact tension specimen of 2124-T351 Aluminium alloy with two types of load sequences as shown in figure 1. In each type of load sequence 10 smaller cycles were inserted in a constant-amplitude loading with a stress ratio of 0.05. In load sequence type 1 S_{max} was kept constant while varying ΔS_b for different tests. The magnitude of S_{min}, which produces equal striation spacings for R = 0.05 cycles and the inserted 10 cycles, was supposed to be S_{op}. For load sequence 1 it was found that S_{op} / S_{max} is equal to 0.2. In the second load sequence the magnitude of S_{min} was kept constant while varying ΔS_b for different tests. If striations of the 10 inserted cycles were invisible, S_{max} of these cycles was supposed to be below S_{op} of the major cycles. If they were visible S_{max} was above S_{op}. The results indicated a high value of S_{op}/S_{max}. However, the results were considered to be inconclusive due to the low number of small cycles [6].

It should be noted that the method of Pelloux et al. is based on the assumption that S_{op} remains constant during the whole load sequence. The same assumption was also made by Sunder and Dash [7], who improved the above mentioned technique by introducing load sequences as shown in figure 2. The load sequences consist of cycles with a constant maximum stress (S_{max}) and a varying minimum stress (S_{min}^{*}). For each subsequent cycle the minimum stress is reduced (or increased) by ΔS_{min} until it reaches the minimum (or maximum) stress of the first cycle. The maximum and minimum stress in the tests were chosen in such a way that $S_{min} < S_{op} < S_{max}$. For cycles with $S_{min}^{*} < S_{op}$ the effective stress range, ΔS_{eff} is assumed to be constant, which should result in a constant striation width. Cycles with $S_{min}^{*} > S_{op}$ should leave striations with an increasing width because of the gradual increase of ΔS_{eff} (and also ΔK_{eff}). By counting the number of striations with equal width, S_{op} can be determined from:

$$S_{min}^{*} < S_{op} < S_{min}^{*} + \Delta S_{min}$$

where S_{min}^{*} is the minimum stress corresponding to the first striations with constant width. Tests on 2024-T3 Aluminium alloy specimens of 3 mm thickness resulted in S_{op}/S_{max} in the range between 0.35 to 0.44. For 5 mm thickness specimens, S_{op} was found to be:

$$0.35 < S_{op} / S_{max} < 0.43 \quad \text{at the surface}$$

$$0.14 < S_{op} / S_{max} < 0.21 \quad \text{at mid thickness}$$

In the present investigation the load sequence developed by Sunder is adopted with the addition of marker load blocks to give an indication of the crack front development.

3 EXPERIMENTAL DETAILS

3.1 Specimens

Specimens were cut from 9.6 mm thick 7075-T6 Aluminium alloy plate material. The material was chosen since it can produce proper marker bands on the fracture surface. Figure 3 illustrates the geometry of the specimen and the initial semi-elliptical notch. Aspect ratios applied were a/c = 1 (semi circular), a/c = 0.8, a/c = 0.6, a/c = 0.4 and a/c = 0.2 (shallow surface notch). The notch was produced by electro spark erosion machining. Mechanical properties of the material are given in figure

3, which also defines the terminology to be used later.

3.2 Load Sequence

The load sequence applied in the present investigation consists of 3 blocks (see figure 4a). The first sub-block corresponds to constant amplitude cycles. This block is the nominal fatigue load on the specimen. The stress ratio in this block was 0.1 and the number of cycles was varied from 300 to 2000, see table 1. S_{op} of this block has to be determined. The second sub-block consists of load cycles with a constant S_{max} and a decreasing S_{min}. In each subsequent cycle in this block S_{min} is reduced by ΔS_{min} until it attains the value of the first block. A useful magnitude of ΔS_{min} in this variable- S_{min} block was determined by a trial and error procedure. ΔS_{min} may not be too small since it would result in a very small change of the striation spacing, which can offer difficulties in the fractographic observations. A too large ΔS_{min} value would impair the accuracy. Considering both restrictions it was found that ΔS_{min} = 3MPa gave good results. The number of cycles with a decreasing S_{min} was in the range of 25 to 90 cycles (table 1). The last block is the marker load block which consists of constant-amplitude cycles with a small ΔS, the same S_{max} as the major cycles and thus a high R-value (R = 0.9). Within the whole block S_{max} was kept constant. The R ratio adopted for the marker loads were based on the experience of Miderhoud [8] and Friedrich and Schijve [9] in testing of corner cracks at open holes and at lug specimens respectively.

Figure 4b illustrates the characteristic pattern of the microfractographs with striations induced by the CA-loading and the decreasing S_{min}, and a strationless area of the marker loads.

In the tests the load block was repeated until specimen failure. Table 1 gives a summary of the tests, which includes the number of cycles in each block, and the initial notch geometry. The crack growth rate was not measured extensively during the test, considering that the marker loads would leave discernible bands on the fracture surface.

4 TEST RESULTS

4.1 Fatigue Lives

The total fatigue lives and the lives until "breakthrough" are given in table 2. Breakthrough occurs when the semi-elliptical surface crack reaches the opposite specimen surface. The crack then is no longer a part-through crack, but a through crack instead. The crack growth life left after breakthrough was relatively short in all tests. The crack propagation curves for the surface (crack length c) and in the thickness direction (crack length a) are given in figure 5.

4.2 Fractographic Observations

4.2.1 Macroscopic observations

Figure 6 shows a typical fracture surface with white bands of marker loads, which represent the crack fronts after a certain number of cycles. The width of the widest marker bands were found to be less than 0.2 mm. Close to the front surface the bands are not very clear. However, the shape of the crack fronts can still be recorded on an optical profile measuring machine at a magnification of 10x (see results in figure 7). Close to the initial notch the marker band was not visible on the profile measuring machine.

In the SEM the position of the marker bands was first located with the aid of the records from the optical profile measuring machine. Marker bands close to the initial notch can still be observed in the SEM, only the first few bands could not be detected. It should be noted that observations in the SEM were restricted to half of the semi-ellipse.

Results are presented in figure 7 which also shows ellipses fitted to the measured crack fronts using the least square method. For crack fronts close to the initial notches 12 to 17 points were used in the fitting procedure, while for larger cracks up to 32 points were used for each crack front. It can be seen that the shape is very close to an ellipse except near to the front surface.

4.2.2 Crack opening stress measurements

Not all specimens did show striations sufficiently well defined for crack opening stress measurements. For specimens PCA1, PCA3, and PCA4, PCA5, and PCA7 the stress level or the S_{min} increment in the crack opening measurement block was too small to induce a discernible striation gradient for S_{op} measurement. In specimen PCA10 with a high fatigue load the crack growth rate was too high, which produced a very rough fracture surface unsuitable for striation observation.

A typical SEM micrograph is shown in figure 8. It shows striations induced by constant-amplitude cycles with equal-spacing striations. The decreasing-S_{min} cycles left striations with gradually increasing width. Marker loads did not induce striations on the fracture surface. S_{op} was determined by counting the number of constant width striations of the decreasing-S_{min} block. The value of S_{op} should be between S_{min} of the first striation with equal width and the preceding S_{min} i.e.

$$S_{min}^{\bullet} < S_{op} < S_{min}^{\bullet} + \Delta S_{min}$$

where $S_{min}^{\bullet}$ is the minimum stress of the first striation with equal spacing. As a first approximation the mean value of these two stresses is taken as S_{op}.

For each specimen more than 100 measurements of S_{op} were made. A summary of the fractographic

observations is given in Appendix 1. It contains interpolated S_{op} values for 6 points along the averaged crack front between two successive marker bands (figure A1) defined by the angle ϕ (figure 3), i.e. for ϕ = 15°,30°,45°,60°,75°,90° respectively. These S_{op}-values were used to calculate ΔK_{eff}, which was related to the average crack growth rate between two marker bands. Complete results of S_{op} measurements along the marker bands can be found in [10].

The curves of S_{op} as a function of the normalized crack depth (a/t) are shown in figure 9. Figure 10 illustrates S_{op} as a function of the angle ϕ at different a/t. These figures show the development of S_{op} during crack extension along the crack front. Some tendencies can be observed in these figures i.e.:

1.In general S_{op} close to the specimen surface (ϕ = 15°) is higher than at any other larger angle ϕ (figure 10). Exceptions are found for the more shallow notches.

2.During crack extension the S_{op} value for a constant angle ϕ develops to a maximum followed by a subsequent decrease near breakthrough (figure 9).

4.2.3 Crack growth near to the front surface

Observations of the microscopic crack growth direction near the specimen front surface show a general tendency: the direction is not parallel to the surface. It makes a negative angle relative to the surface (see figure 11). At a larger angle (>15°) the local crack growth direction is more or less perpendicular to the crack front curvature.

4.3 Crack Growth Rate and Crack Shape Development

The crack growth rate for a specific angle ϕ is determined from the perpendicular distance between successive crack fronts (marker bands) divided by the number of constant-amplitude cycles. This procedure results in average crack growth rate between two successive crack fronts (see figure A1 in the Appendix).

The crack growth rate as a function of the normalized crack depth (a/t) at different angles ϕ is given in figure 12. The figures show that initially da/dN is larger at the deepest point (ϕ = 90°) for the shallow notches (figure 12, specimen PCA6 and PCA15). However, after some crack extension the crack growth rate near the surface (ϕ = 15°) predominates, and da/dN is lower for larger angles ϕ with a minimum at the deepest point (ϕ = 90°). The shallow initial notch shows an exceptional behaviour because most crack extension occurs at the deepest point (see figure 7). The crack initially did not grow at the front surface, but it initiated at the notch periphery at the deepest point and then grew along the border of the notch until it reached the front surface.

For a more universal presentation of the crack growth rate, da/dN has been plotted as a function of the stress intensity range ΔK and ΔK_{eff}. For this purpose the Newman-Raju solution [11] for semi-elliptical cracks was adopted, because the shape of the crack fronts are very close to a

semi-ellipse, except near the surface where the crack fronts trails behind. The crack depth a, and crack length c for the Newman-Raju solution were obtained by fitting ellipses to the crack fronts, excluding points near to the front surface. The least square fitting has been mentioned before. The Newman-Raju solution for K is given in Appendix 2.

ΔK was calculated for the average elliptical crack fronts between two successive marker bands (see figure A1). Figure 13 illustrates the crack growth rate at different angles as a function of ΔK and ΔK_{eff}. The solid lines in the figures represent the Paris equation for the crack growth rate of through cracks (C = 2.29*10E-4 and m = 2.88 for da/dN as a function of ΔK for R=0.1, and C = 4.36*10E-4 and m = 2.88 for da/dN as a function of ΔK_{eff}. The constants of the Paris equation were obtained in preliminary crack growth tests using the same 9.6mm thick Al 7075-T6 plate specimens with through cracks. The stress ratio R was equal to 0.1. S_{op} of the through cracks was measured with an extensometer placed close to the crack tip. The crack growth rate was plotted as a function of ΔK and ΔK_{eff}. The least square method was used to obtain the constants of the Paris equation.For the part-through cracks ΔK_{eff} was calculated by replacing S with S_{max} - S_{op} in the Newman-Raju solution. A comparison between the results of the through cracks and the part-through cracks is made in figure 13. It can be seen that for lower ΔK-values the crack growth rate of part-through cracks for all ϕ-values is higher than for through cracks, although the R ratio is the same (R=0.1). At a higher ΔK the points are scattered around the Paris equation.

The da/dN vs ΔK_{eff} relation shows that for low ΔK_{eff}-values the measured crack growth rate at different angle ϕ is scattered around the Paris equation line (C = 4.36*10E-4 and m = 2.88). For higher angles ϕ (ϕ = 60 °, 75°, 90°) and higher ΔK_{eff} the crack growth rate is lower.

The crack shape development curves (a/c as a function of a/t) are shown in figure 14. These curves follow a similar tendency as found in other investigations for similar initial notches [e.g. 12,13]. A crack with a low initial aspect ratio (specimen PCA6 with a/c = 0.2) grows towards a more semi-circular shape, but it does not have the opportunity to develop to the semi-circular shape and attains a final a/c ≈ 0.57. Specimen PCA15 with a/c = 0.4 grows to final a/c ≈ 0.7. Cracks with higher initial aspect ratio first grow to a higher aspect ratio, but soon a/c starts to decrease towards a final a/c ≈ 0.70.

5 DISCUSSION

5.1 Crack Opening Stress Level

Figures 9 and 10 illustrate that S_{op} on the average appears to be fairly low. S_{op}/S_{max} values vary from 0.1 to 0.29 with 0.2 as a typical average value. It is easily derived that:

$$U = \frac{\Delta S_{eff}}{\Delta S} = \frac{1 - S_{op}/S_{max}}{1 - R}$$

$S_{op}/S_{max} \approx 0.2$ implies for R=0.1 (present test series) that $\Delta S_{eff}/\Delta S = 0.9$. In other words the amount of crack closure is rather limited. The low crack closure level can be explained by recalling that:

1. The state of stress is predominantly plane strain due to the thick specimen used.

2. The yield stress of the material (7075-T6) is high ($S_{0.2} = 509$ MPa).

Both resulting in a small plastic zone around the crack tip. The plastic zone size can be estimated with equation 1:

$$r_p = \frac{1}{\pi\alpha}\left(\frac{K}{S_{0.2}}\right)^2$$

With $\alpha = 3$ and $S_{0.2} = 509$ MPa, a point at mid thickness with a=4.8mm and c=5.5mm gives $r_p = 0.03$ mm, whis is indeed a small value compared to the crack size.

The constant-amplitude data for through cracks mentioned before indicate $S_{op}/S_{max} \approx 0.28$. Although that is somewhat higher than for the part-through cracks, it is still a very low crack opening stress level. It is interesting to recall that results of Sunder and Dash discussed before. They found $0.14 < S_{op}/S_{max} < 0.21$ at mid thickness of 2024-T3 (t=5mm, $R \approx 0$), but a higher value $0.35 < S_{op}/S_{max} < 0.43$ at the surface. The higher S_{op} at the material surface is generally attributed to more plastic deformation (plane stress) at the surface. It implies that the large plastic zone will increase S_{op} at the surface, and at the same time reduce S_{op} away from the surface due to propping effect. Three-dimensional finite element calculations by Chermahini et al. [14] on through crack specimens confirms the higher S_{op} at the surface.

5.2 The Ligament Effect

It is generally accepted that the occurrence of crack closure is predominantly related to the plastic zone in the wake of the crack. Under special conditions other mechanisms (crack surface mismatch and surface oxidation) may also contribute to crack closure, but they will not be considered here. During variable amplitude loading a plastic zone ahead of the crack tip induced by a high load will open the

semi-ellipse, except near the surface where the crack fronts trails behind. The crack depth a, and crack length c for the Newman-Raju solution were obtained by fitting ellipses to the crack fronts, excluding points near to the front surface. The least square fitting has been mentioned before. The Newman-Raju solution for K is given in Appendix 2.

ΔK was calculated for the average elliptical crack fronts between two successive marker bands (see figure A1). Figure 13 illustrates the crack growth rate at different angles as a function of ΔK and ΔK_{eff}. The solid lines in the figures represent the Paris equation for the crack growth rate of through cracks (C = 2.29*10E-4 and m = 2.88 for da/dN as a function of ΔK for R=0.1, and C = 4.36*10E-4 and m = 2.88 for da/dN as a function of ΔK_{eff}. The constants of the Paris equation were obtained in preliminary crack growth tests using the same 9.6mm thick Al 7075-T6 plate specimens with through cracks. The stress ratio R was equal to 0.1. S_{op} of the through cracks was measured with an extensometer placed close to the crack tip. The crack growth rate was plotted as a function of ΔK and ΔK_{eff}. The least square method was used to obtain the constants of the Paris equation.For the part-through cracks ΔK_{eff} was calculated by replacing S with S_{max} - S_{op} in the Newman-Raju solution. A comparison between the results of the through cracks and the part-through cracks is made in figure 13. It can be seen that for lower ΔK-values the crack growth rate of part-through cracks for all ϕ-values is higher than for through cracks, although the R ratio is the same (R=0.1). At a higher ΔK the points are scattered around the Paris equation.

The da/dN vs ΔK_{eff} relation shows that for low ΔK_{eff}-values the measured crack growth rate at different angle ϕ is scattered around the Paris equation line (C = 4.36*10E-4 and m = 2.88). For higher angles ϕ (ϕ = 60 °, 75°, 90°) and higher ΔK_{eff} the crack growth rate is lower.

The crack shape development curves (a/c as a function of a/t) are shown in figure 14. These curves follow a similar tendency as found in other investigations for similar initial notches [e.g. 12,13]. A crack with a low initial aspect ratio (specimen PCA6 with a/c = 0.2) grows towards a more semi-circular shape, but it does not have the opportunity to develop to the semi-circular shape and attains a final a/c ≈ 0.57. Specimen PCA15 with a/c = 0.4 grows to final a/c ≈ 0.7. Cracks with higher initial aspect ratio first grow to a higher aspect ratio, but soon a/c starts to decrease towards a final a/c ≈ 0.70.

5 DISCUSSION

5.1 Crack Opening Stress Level

Figures 9 and 10 illustrate that S_{op} on the average appears to be fairly low. S_{op}/S_{max} values vary from 0.1 to 0.29 with 0.2 as a typical average value. It is easily derived that:

$$U = \frac{\Delta S_{eff}}{\Delta S} = \frac{1 - S_{op}/S_{max}}{1 - R}$$

$S_{op}/S_{max} \approx 0.2$ implies for R=0.1 (present test series) that $\Delta S_{eff}/\Delta S = 0.9$. In other words the amount of crack closure is rather limited. The low crack closure level can be explained by recalling that:

1. The state of stress is predominantly plane strain due to the thick specimen used.

2. The yield stress of the material (7075-T6) is high ($S_{0.2}$ = 509 MPa).

Both resulting in a small plastic zone around the crack tip. The plastic zone size can be estimated with equation 1:

$$r_p = \frac{1}{\pi\alpha}\left(\frac{K}{S_{0.2}}\right)^2$$

With α = 3 and $S_{0.2}$ = 509 MPa, a point at mid thickness with a=4.8mm and c=5.5mm gives r_p=0.03 mm, whis is indeed a small value compared to the crack size.

The constant-amplitude data for through cracks mentioned before indicate $S_{op}/S_{max} \approx 0.28$. Although that is somewhat higher than for the part-through cracks, it is still a very low crack opening stress level. It is interesting to recall that results of Sunder and Dash discussed before. They found $0.14 < S_{op}/S_{max} < 0.21$ at mid thickness of 2024-T3 (t=5mm, R $\approx$ 0), but a higher value $0.35 < S_{op}/S_{max} < 0.43$ at the surface. The higher S_{op} at the material surface is generally attributed to more plastic deformation (plane stress) at the surface. It implies that the large plastic zone will increase S_{op} at the surface, and at the same time reduce S_{op} away from the surface due to propping effect. Three-dimensional finite element calculations by Chermahini et al. [14] on through crack specimens confirms the higher S_{op} at the surface.

5.2 The Ligament Effect

It is generally accepted that the occurrence of crack closure is predominantly related to the plastic zone in the wake of the crack. Under special conditions other mechanisms (crack surface mismatch and surface oxidation) may also contribute to crack closure, but they will not be considered here. During variable amplitude loading a plastic zone ahead of the crack tip induced by a high load will open the

crack and thus reduce the crack opening stress. In this case the crack opening stress is not only dependent upon the plastic zone in the wake of the crack but also on the large plastic zone ahead of the crack. An extreme case where the crack opening stress level is influenced by the plastic zone ahead of the crack is the occurrence of net section yield. Since net section yield involves large plastic deformation ahead of the crack, it can reduce the crack opening stress. The occurrence of net section yield can occur under CA loading later in the life i.e. when the crack length is large, leaving a small ligament to carry the load.

The development of S_{op} for a constant ϕ as shown in figure 9 can be explained with the occurrence of net section yield. At the beginning of the crack extension the lower S_{op} is caused by the absence of a plastic zone in the wake of the crack. As the crack extends, plastic deformation left in the wake of the crack also develops resulting in an increasing S_{op}. After some growth in the thickness direction the ligament size becomes smaller with a corresponding decrease of restraint to plastic deformation in the ligament. When the plastic zone reaches the back surface net-section yield occurs. Due to the large plastic deformation induced by the net-section yielding the crack surface contact is reduced, resulting in a lower S_{op}. The crack depth at the occurrence of the net-section yielding can be roughly estimated by assuming that the ligament area (see figure 3) carries the yield stress, and the cross sectional area far from the crack (i.e. outside the ligament) carries the nominal stress:

$$S_{0.2}(t.2c - \pi ac/2) = S_{max}(t.2c) \quad \text{or } a/t = 4/\pi\,(1 - S_{max}/S_{0.2})$$

Substitution of S_{max} and S_{op} gives a = 8.6 mm or a/t = 0.9. Figure 9 shows that the S_{op} started to decrease at $a/t \approx 0.6$ for specimens PCA2, PCA14, and PCA13 and $a/t \approx 0.75$ for specimen PCA15. This discrepancy might be caused by the fact that the growth of the plastic deformation leading to the net-section yielding does not take place abruptly but progressively. The deviations also arise from the rough estimate in the above equation, however it is believed that it gives a correct order of magnitude which supports the net section yield idea.

5.3 Crack Growth Rate

Due to different stress intensities along the crack front of semi-elliptical cracks it is expected that the crack growth rate will vary accordingly. Different K along the crack front will induce different plastic zone sizes, which will result in a variation of crack closure along the crack front. By taking into account the crack closure variation along the crack front it was hoped that ΔK_{eff} of individual points along the crack periphery will be similar to corresponding ΔK_{eff} of through cracks. However, figure 13 shows that similar ΔK_{eff} values for surface cracks and through cracks give similar crack growth rate only in limited range of ΔK_{eff}. Deviation occurs mainly at ϕ = 60°, 75°, 90°. For high ΔK_{eff} values and these angles, a slower crack growth rate is found as compared to through crack data.

The large plastic deformation in the ligament should be expected to have influence on the crack tip geometry. The vacuum infiltration technique was developed by Bowles [15] to study crack tip geometry. It revealed that even at minimum load the crack tip was microscopically blunt. The occurrence of net section yielding should induce more opening at the crack tip,but also more blunting. The crack tip blunting will reduce the stress intensity at the crack tip which in turn will reduce the crack extension.

5.4 Crack Shape Development

The crack shape development curves (a/c vs a/t), figure 14, follow the same tendency as found in the literature [e.g. 12 and 13] The increase of a/c at the beginning is caused by higher crack growth rates at the deepest part of the crack. For cracks with larger a/c ratios the initially higher crack growth rate at the deepest point occurred only for a short time i.e. a small amount of crack extension up to a/t = 0.3 - 0.4 (see figure 12, specimens PCA2 and PCA13). For shallower cracks it occurred up to a/t 0.5 - 0.6 (figure 12, specimens PCA6 and PCA15). During further crack extension the crack growth rate near to the surface is always higher than at the deepest point, which results in a later decrease of a/c. Apparently for all initial notches there is a tendency of the a/c development curves to converge to a similar value. Due to the limited thickness of the material that value can not be reached.

6 CONCLUSIONS

Crack growth from semi-elliptical fatigue cracks in 7075-T6 plate material (9.6 mm) under constant amplitude loading(R=0.1) was studied by a fractographic analysis. Semi-elliptical starter notches with a different shallowness were adopted: a/t=1(semi-circular), 0.8, 0.6, 0.4, and 0.2(very shallow). Marker loads were used to study the crack front development. Small batches of cycles with a decreasing S_{min} were introduced to determine S_{op} from striation spacing measurements. The main results are summarized below:

1. During crack growth the shape of the semi-elliptical crack remains approximately semi-elliptical, but the shape (aspect ratio a/c) changes. The change of a/c agrees with the trend predicted by the K-variation along the crack front, semi-circular cracks become more shallow, and very shallow cracks become less shallow.

2. The crack closure level S_{op} varies along the crack front. In general it is relatively low ($\Delta K_{eff}/\Delta K$ from 0.79 to 1.00), which is associated with the plane strain conditions and the high yield stress. More closure occurred at the specimen surface (plane stress effect). A remarkable observation is that S_{op} is reducing at the deepest point of the crack if the crack is relatively (a/t) deep. This is attributed to an increasing size of the plastic zone ahead of the crack with a tendency to net section yield in the ligament material near the deepest point of the crack.

3. The agreement of the $da/dN = f(\Delta K_{eff})$ curves for surface cracks and for through cracks was only found for a limited range of the crack depth. At a higher crack depth the crack growth rate of surface cracks is generally lower than for through cracks. It is believed that this tendency is caused by the violation of the similitude requirement that the plastic zone infront of the crack must be much smaller than the ligament.

REFERENCES

1. Elber,W.'Fatigue crack closure under cyclic tension' Engineering Fracture Mechanics vol.2 no.1(1970) pp. 37-46.
2. Schijve,J.'Fatigue crack closure, observations and technical significance' Report LR-485, Department of Aerospace Engineering, Technical University Delft, April 1986.
3. Ewalds,H.L.,and Furnee,R.T.,'Crack closure measurement along the fatigue crack front on centre cracked specimens' International Journal of Fracture 14(1978) pp. R53-R55.
4. Fleck,N.A.,and Smith,R.A.'Crack closure is it just a surface phenomenon ?' International Journal of Fatigue, July 1982, pp. 157-160.
5. Shaw,W.J.D.,and Le May,I.,'Crack closure during crack propagation' Fracture Mechanics, ASTM STP 677, C.W.Smith,Ed.,American Society for Testing and Materials, 1979, pp. 233-246.
6. Pelloux,R.M.,Faral,M.,McGee,W.M.,'Fractographic measurements of crack tip closure' Fracture Mechanics: Twelfth Conference, ASTM STP 700, American Society for Testing and Materials, 1979, pp. 35-48.
7. Sunder,R.,Dash,P.K.,'Measurement of fatigue crack closure through electron microscopy' International Journal of Fatigue, April 1982, pp. 97-105.
8. Minderhoud,S.,'Fatigue crack growth of corner cracks' Thesis of the Department of Aerospace Engineering, Delft University of Technology, June 1982.
9. Friedrich,S.,and Schijve,J.,'Fatigue crack growth of corner cracks in lug specimens' Report LR-375, Department of Aerospace Engineering, Delft University of Technology, January 1983.
10. Ichsan, S.P.,'Compilation of crack opening stress measurements on 7075-T6 sheet specimen with semi-elliptical surface crack under constant amplitude loading' Subject group Materials and Production Processes, Department of Aerospace Engineering, Delft University of Technology 1989.

11. Newman,J.C.,Jr.,and Raju,I.S.,'Stress-intensity factor equation for crack in three-dimensional finite bodies subjected to tension and bending loads' Fracture Mechanics: Fourteenth Symposium. Vol.1: Theory and Analysis, ASTM STP 791, J.C.Lewis and G.Sines, Eds pp. 238-265.

12. Gorner,F.,Mattheck,C.,Munz,D.,'Change in geometry of surface cracks during alternating tension and bending' Z.Werkstofftechniek,no.14(1983), pp. 11-18.

13. Vosikovsky,O.,and Rivard,A.,'Growth of surface fatigue cracks in a steel plate' International Journal of Fatigue, July 1981, pp. 111-115.

14. Chermahini,R.G.,Shivakumar,K.N.,Newman,J.C.,Blom,A.F.,'Three-dimensional aspects of plasticity-induced fatigue crack closure' Engineering Fracture Mechanics, Vol.34, No.2, pp.393-401, 1989.

15. Bowles,C.Q.,'The role of environment, frequency, and wave shape during fatigue crack growth in Aluminum alloys' Department of Aerospace Engineering, Delft University of Technology, Report LR-270, 1978.

	initial notch		constant-amplitude block			crack-opening measurement		marker load		
spec. Number	a (mm)	2c (mm)	S_{max} (MPa)	S_{min} (MPa)	number of cycles	ΔS_{min} (MPa)	number of cycles	S_{max} (MPa)	S_{min} (MPa)	number of cycles
PCA1	1.92	6.40	120	12	1000	4.5	24	120	108	40000
PCA2	1.92	6.40	150	15	1000	3	45	150	135	30000
PCA3	1.92	6.40	85	8.5	2000	3	25	85	70	40000
PCA4	1.92	6.40	100	10	1500	3	30	100	85	40000
PCA5	1.92	19.2	120	12	1000	2.5	43	120	108	40000
PCA6	1.92	19.2	150	15	1000	3	45	150	135	30000
PCA7	1.92	19.2	150	15	500	1.5	90	150	140	30000
PCA10	1.92	6.4	180	18	300	3	54	180	158.4	25000
PCA13	1.92	3.84	150	15	1000	3	45	150	135	30000
PCA14	1.92	4.8	150	15	1000	3	45	150	135	30000
PCA15	2.88	14.4	150	15	700	3	45	150	135	30000

Table 1. Summary of the test parameters

specimen number	life to breakthrough (cycles)	life to failure (cycles)
PCA1	32000	35000
PCA2	19000	20395
PCA3	110000	120394
PCA4	39020	45020
PCA5	15000	17261
PCA6	8000	8625
PCA7	7000	7694
PCA10	10200	10983
PCA13	24000	24090
PCA14	22000	25170
PCA15	8400	10227

Table 2. Fatigue lives to breakthrough and total fatigue lives

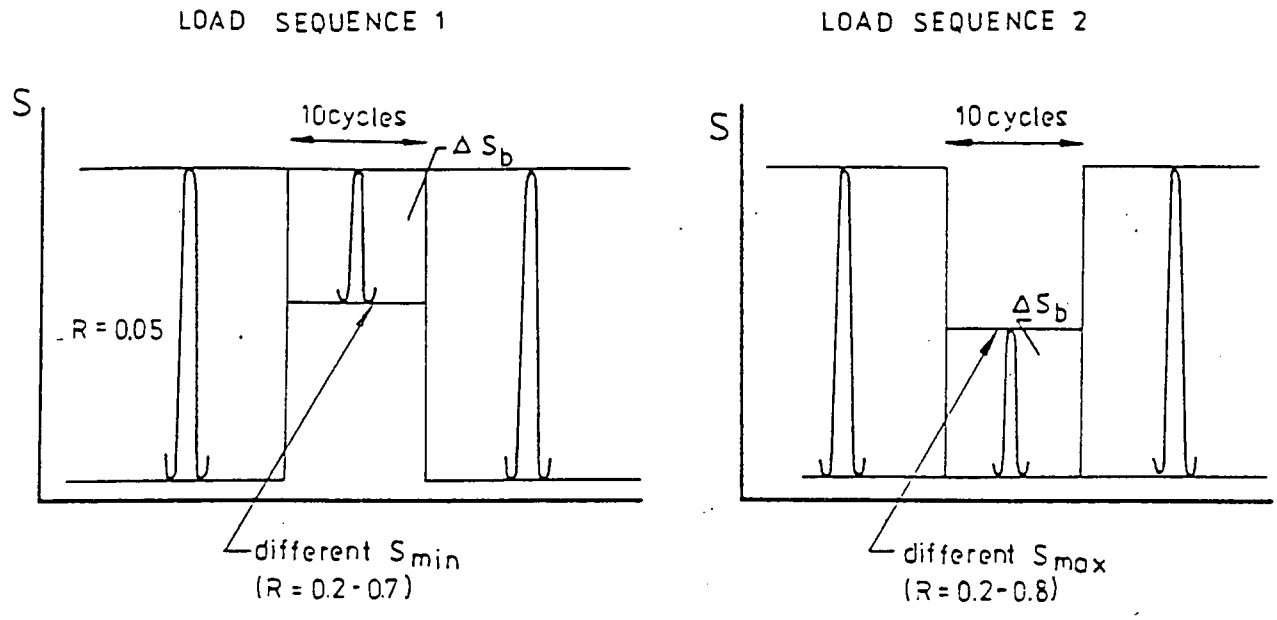

Figure 1. Two types of load sequences applied by Pelloux et al.[6] to determine S_{op}.

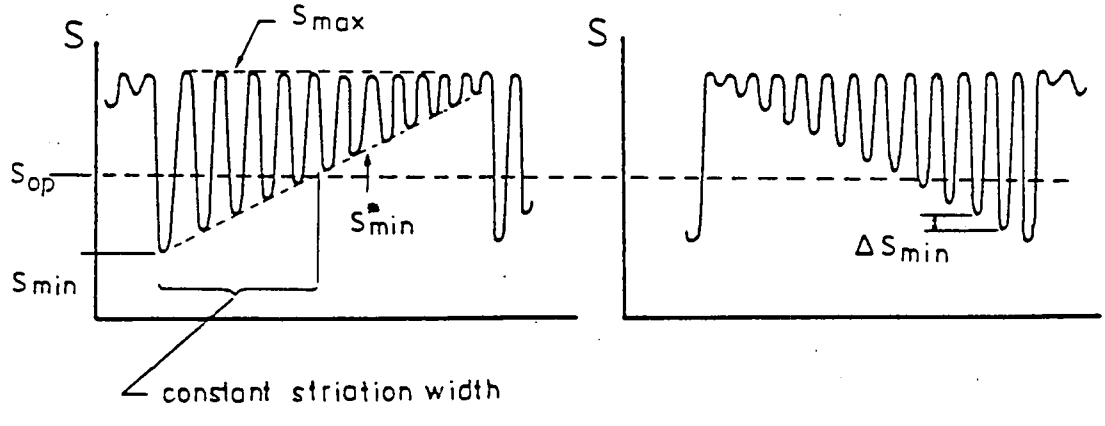

Figure 2. Two types of load sequences with a variable S_{min} applied by Sunder and Dash [7].

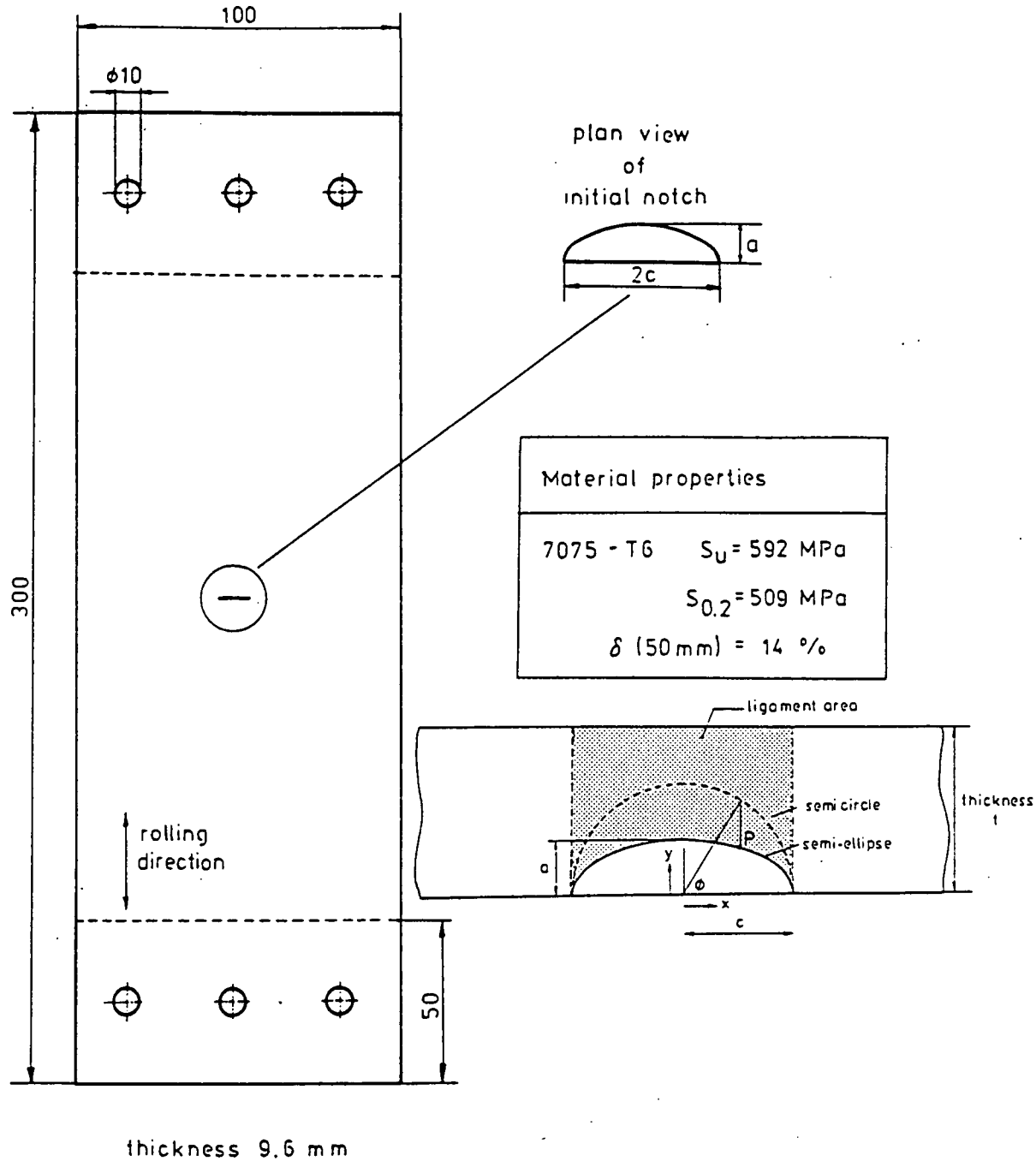

Figure 3. Geometry of the specimen, mechanical properties of the material and definition of the terminology related to surface cracks.

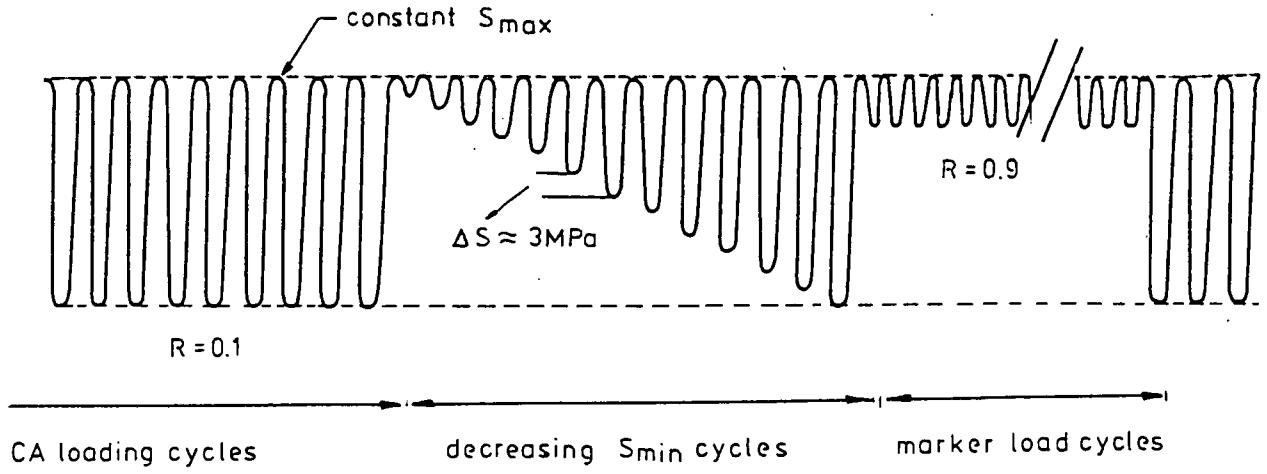

Figure 4a. Load sequence in the present investigation with CA loading cycles, decreasing S_{min} cycles to determine S_{op}, and marker load cycles.

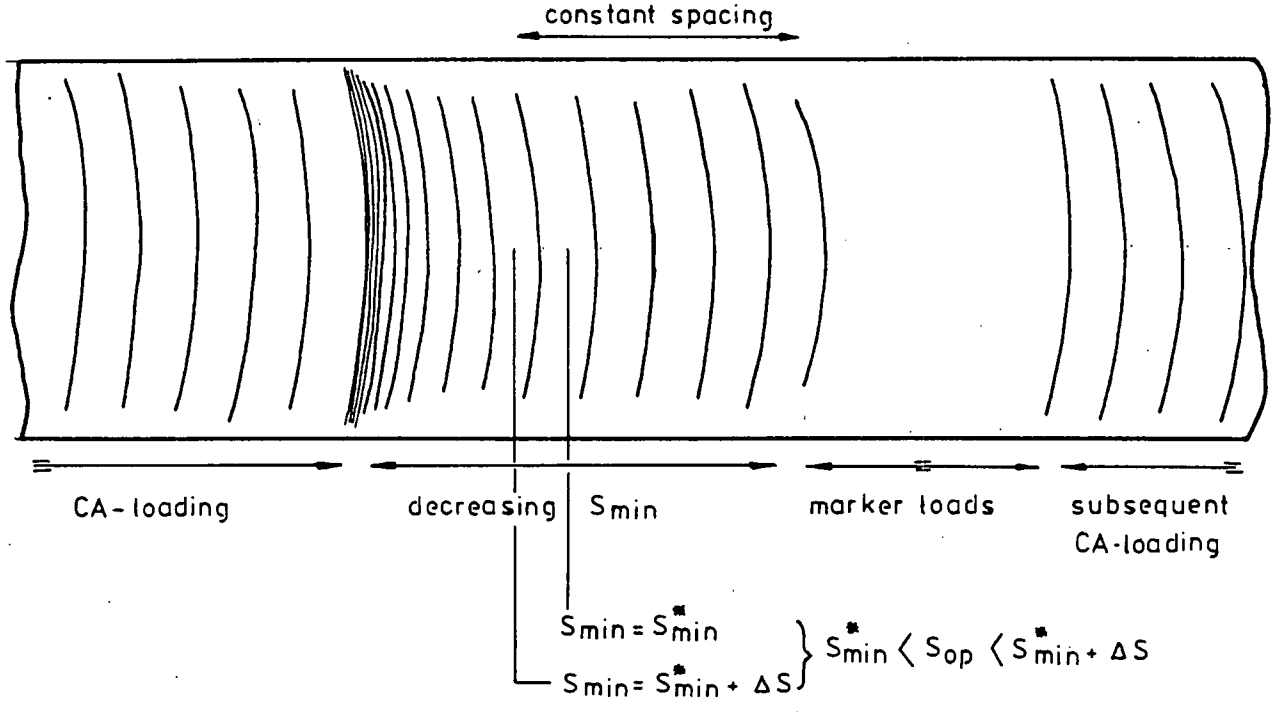

Figure 4b. Characteristic pattern of microfractograph showing striations induced by CA loading, decreasing S_{min} cycles with increasing striation spacing, and striationless area of marker load cycles.

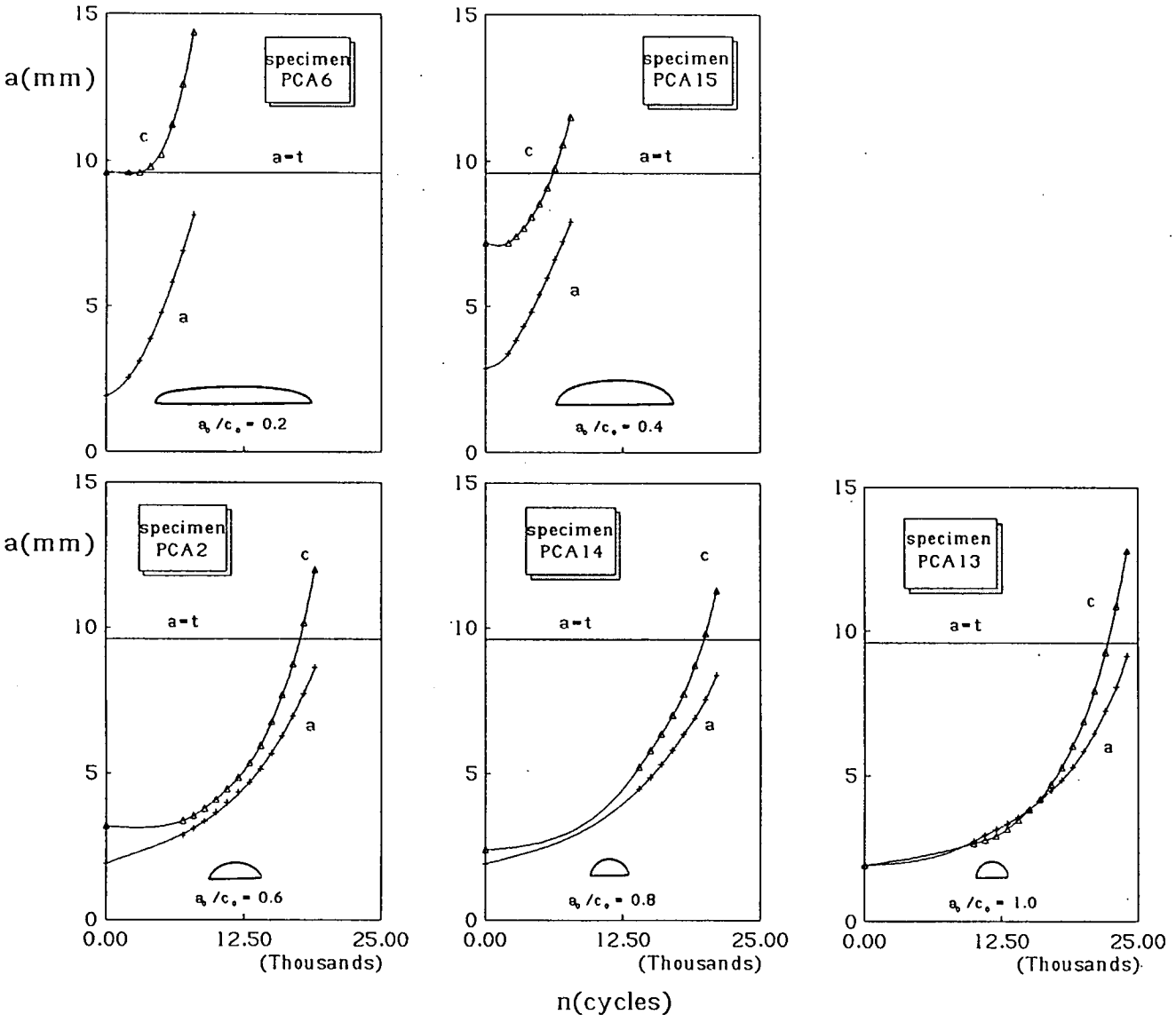

Figure 5. Crack propagation curves on the surface and in the thickness direction.

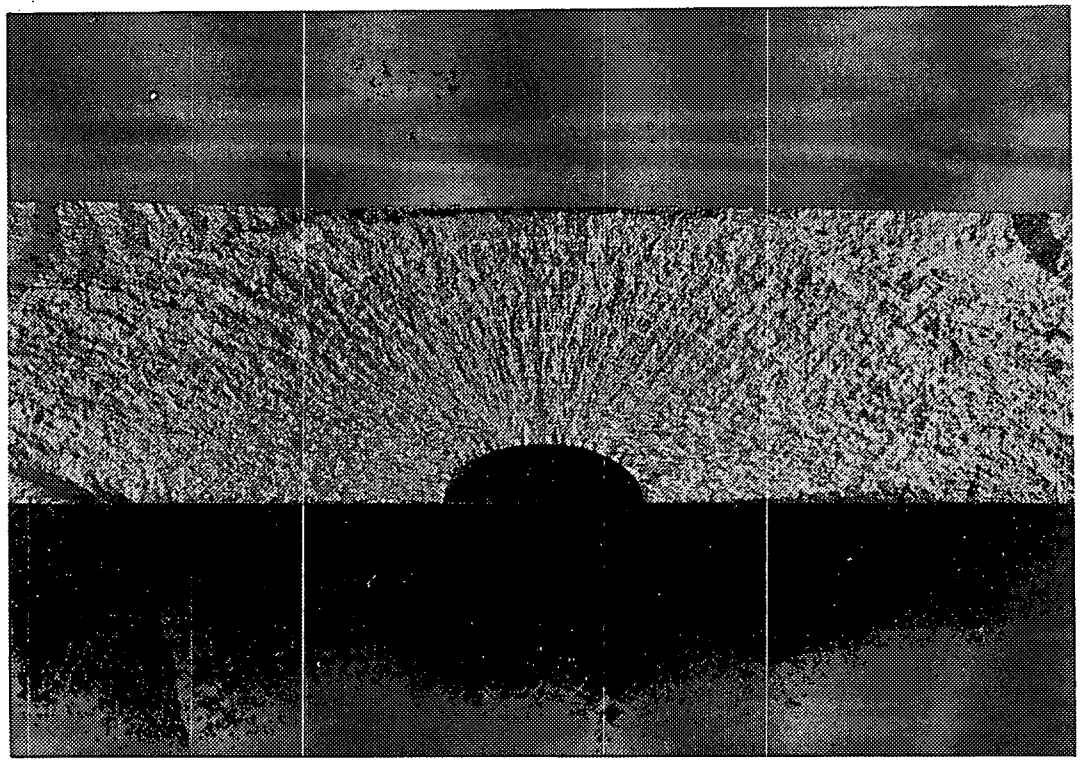

Figure 6. Typical fracture surface with white bands of marker loads (specimen PCA2).

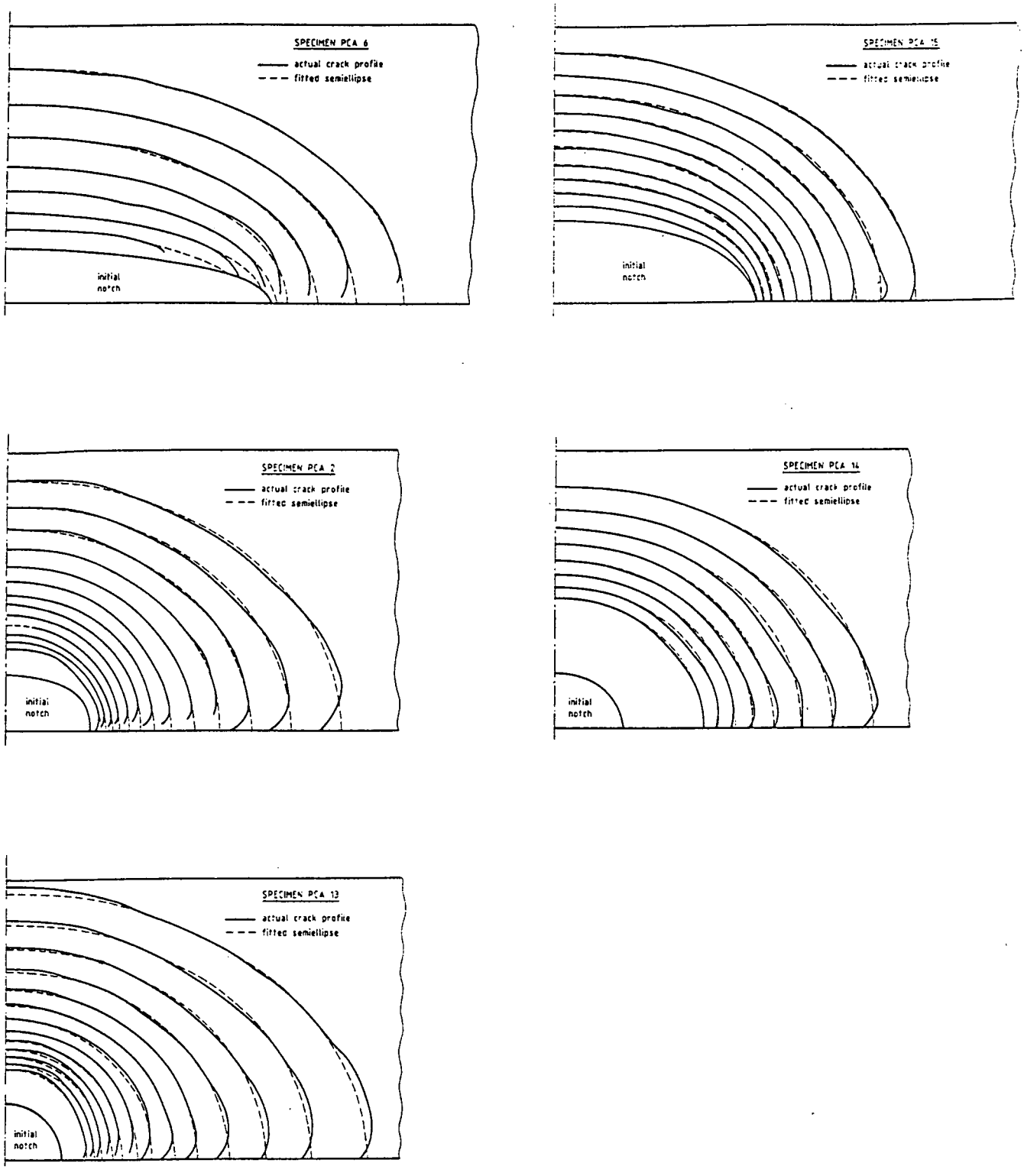

Figure 7. The shape of actual crack profile and fitted semiellipse.

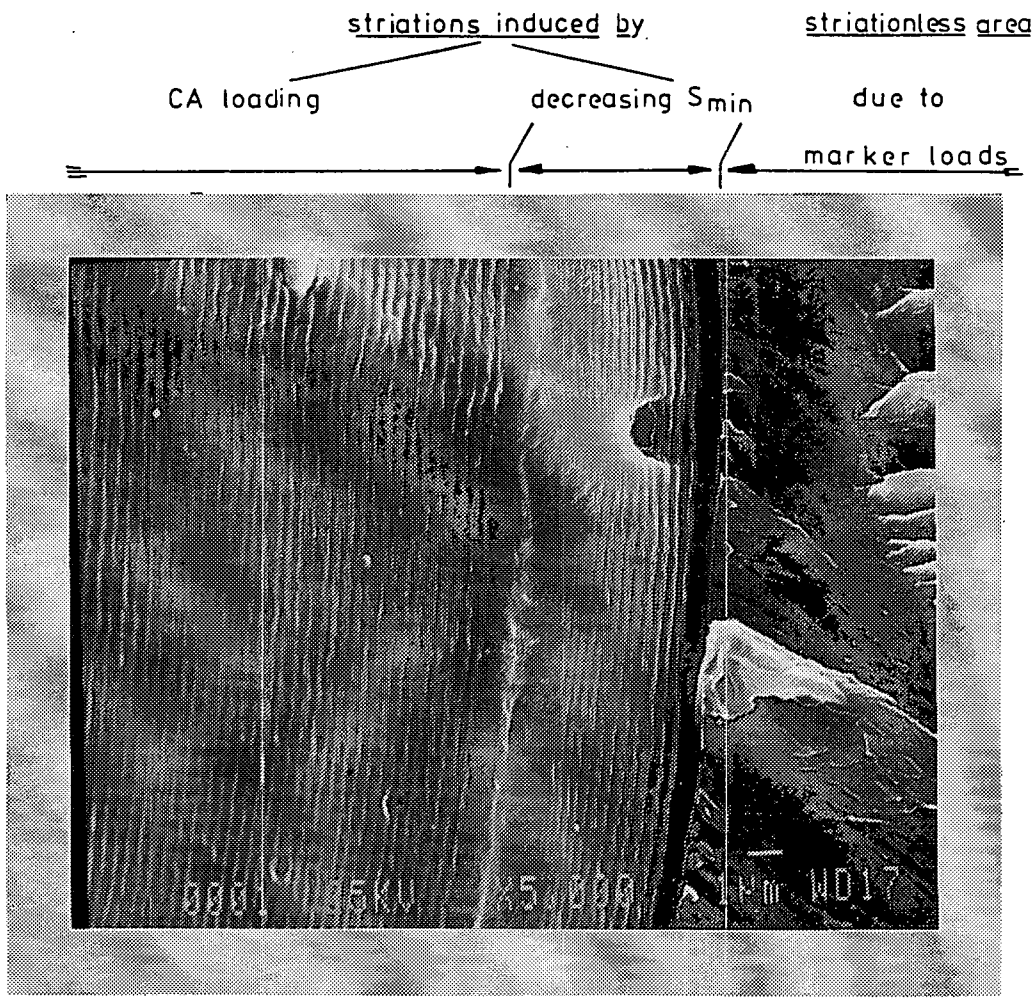

Figure 8. A typical SEM micrograph showing striations induced by CA loading, decreasing S_{min} cycles, and striationless area due to marker cycles.

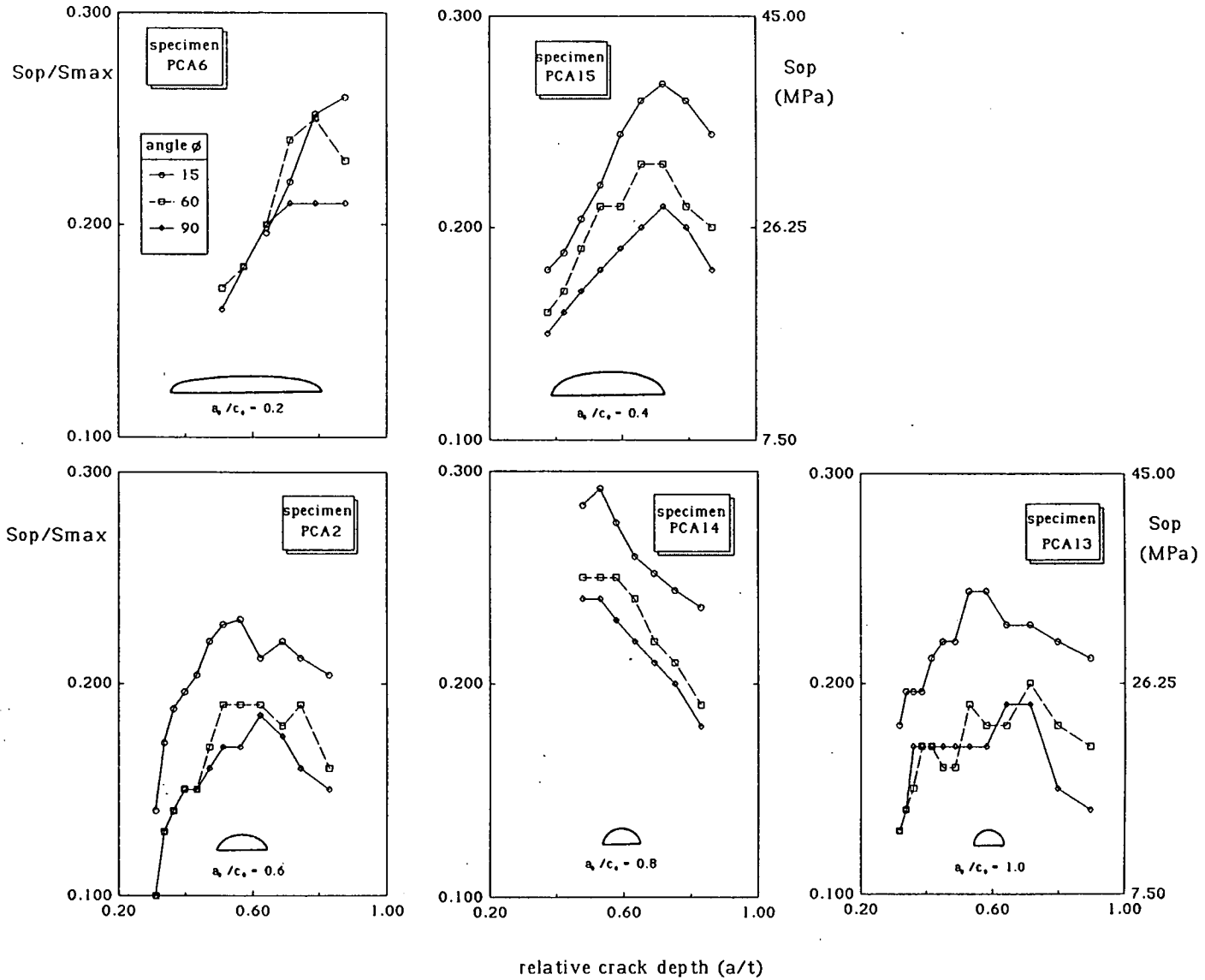

Figure 9. S_{op} as a function of relative crack depth (a/t) at different angles ϕ (for clarity results for only 3 values of ϕ are shown).

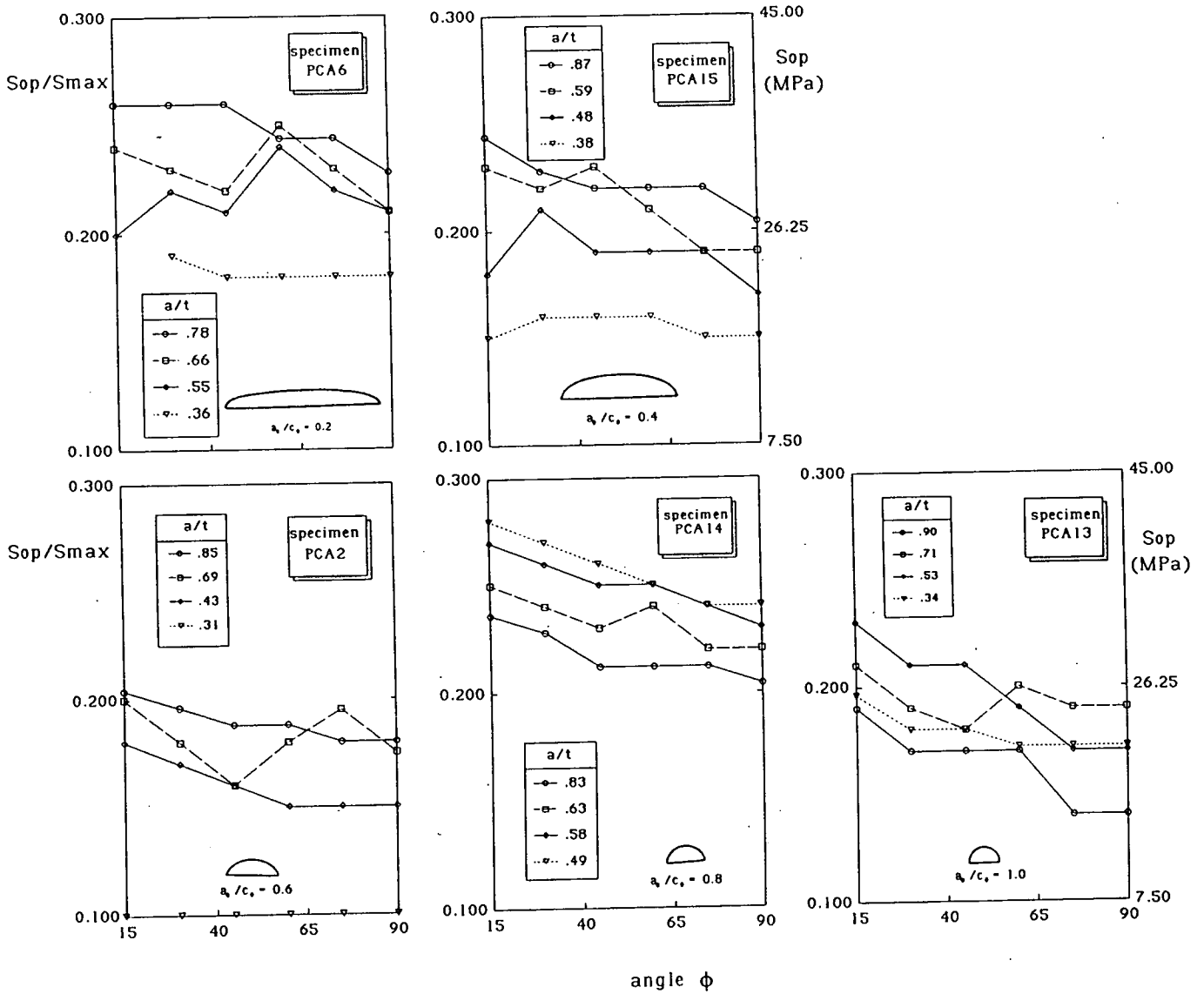

Figure 10. S_{op} as a function of angle ϕ at different crack depth (a/t) (for clarity results for only 4 values of a/t are shown).

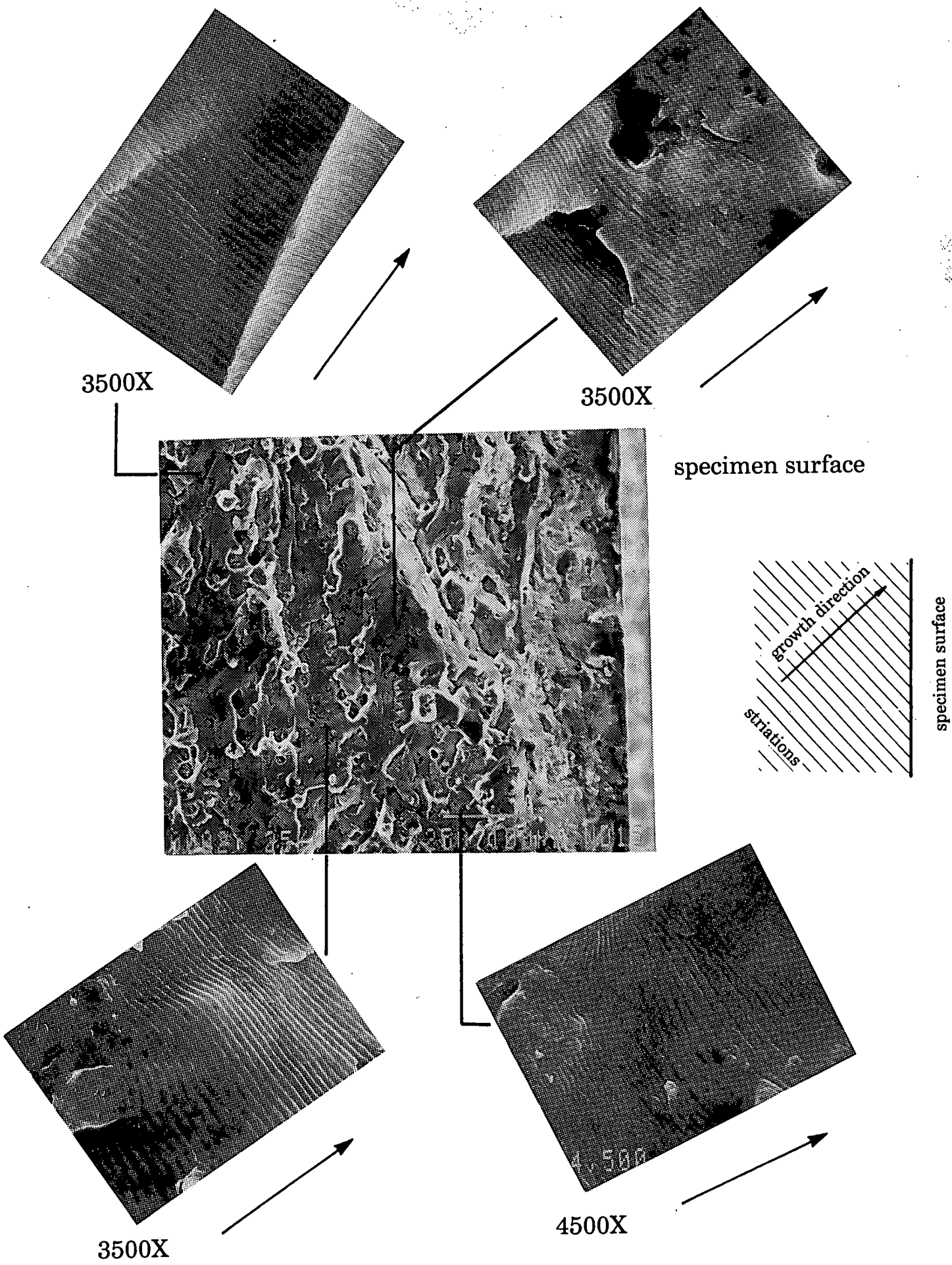

Figure 11. Direction of crack growth close to the specimen surface.

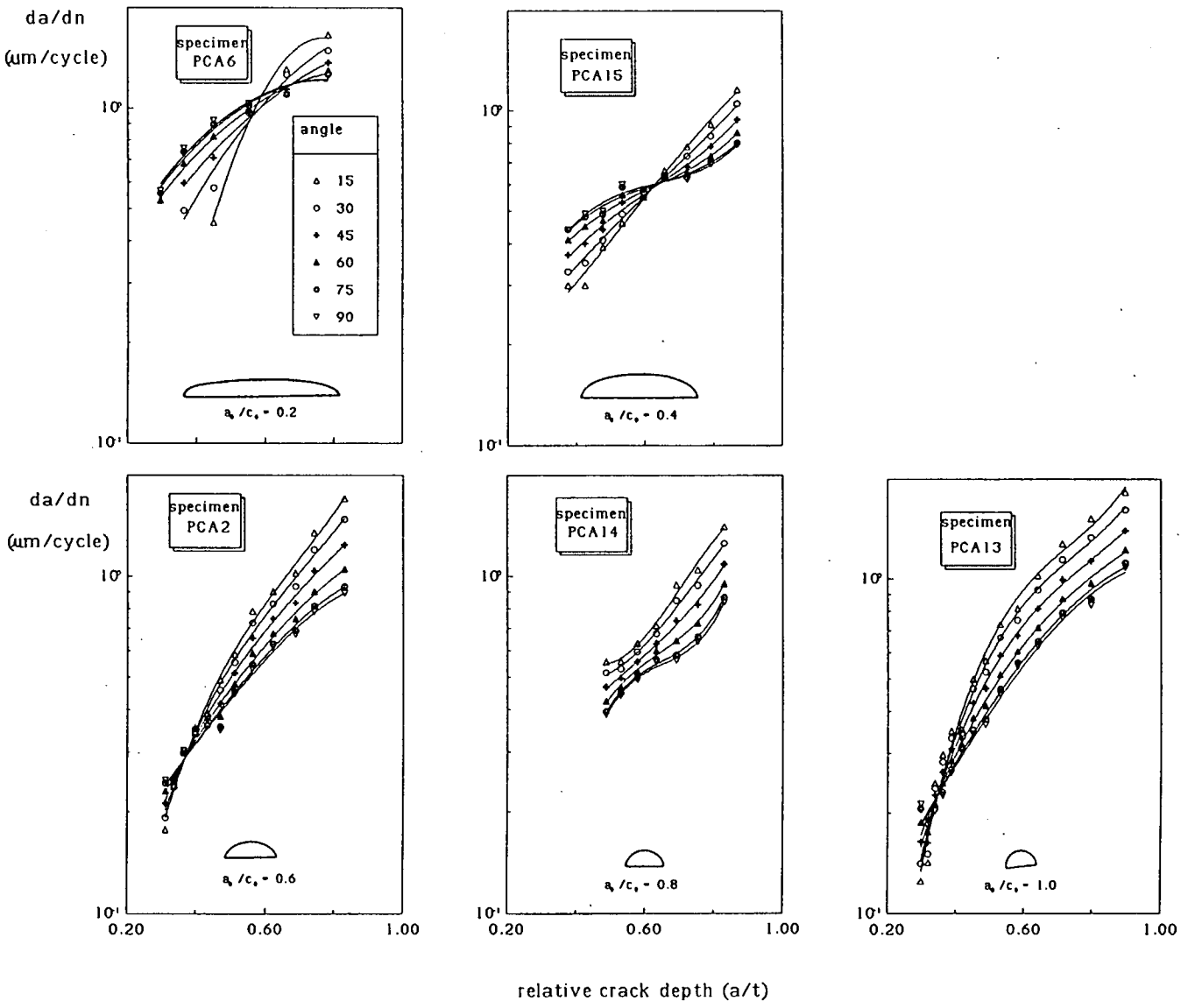

Figure 12. Crack growth rate (da/dN) as a function of relative crack depth (a/t) at different angle ϕ.

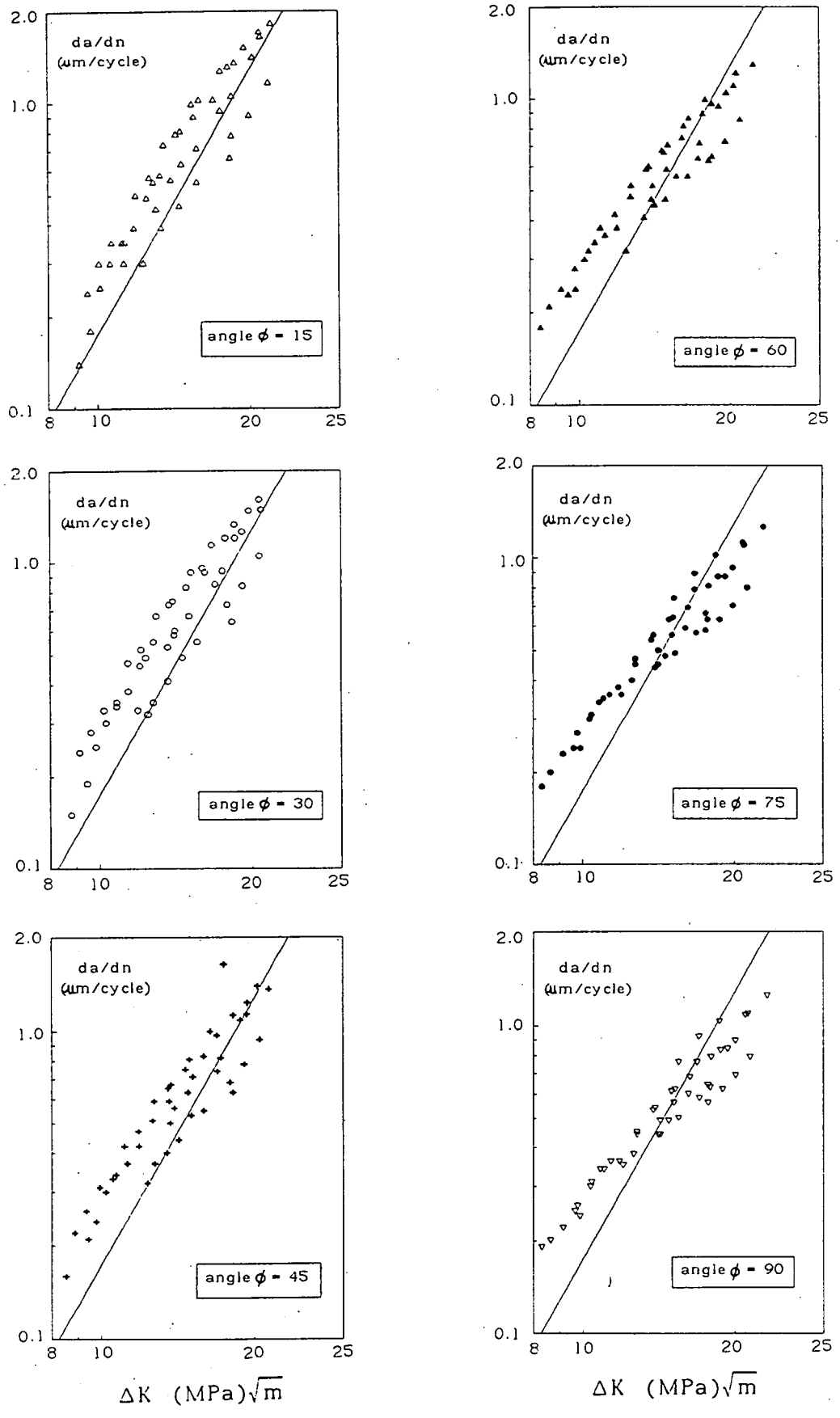

Figure 13a. Crack growth rate (da/dn) as a function of ΔK.

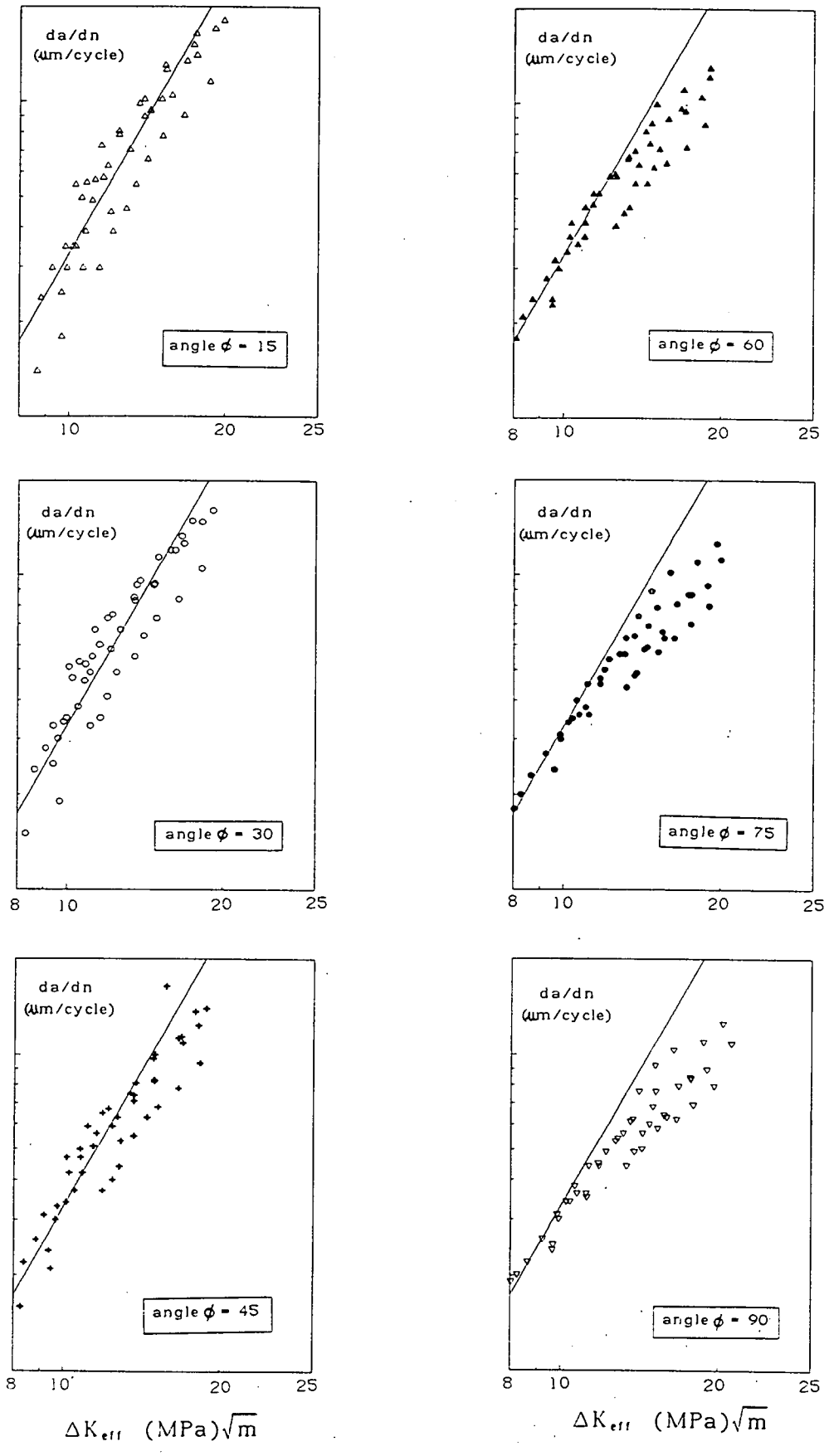

Figure 13b. Crack growth rate (da/dn) as a function of ΔK_{eff}.

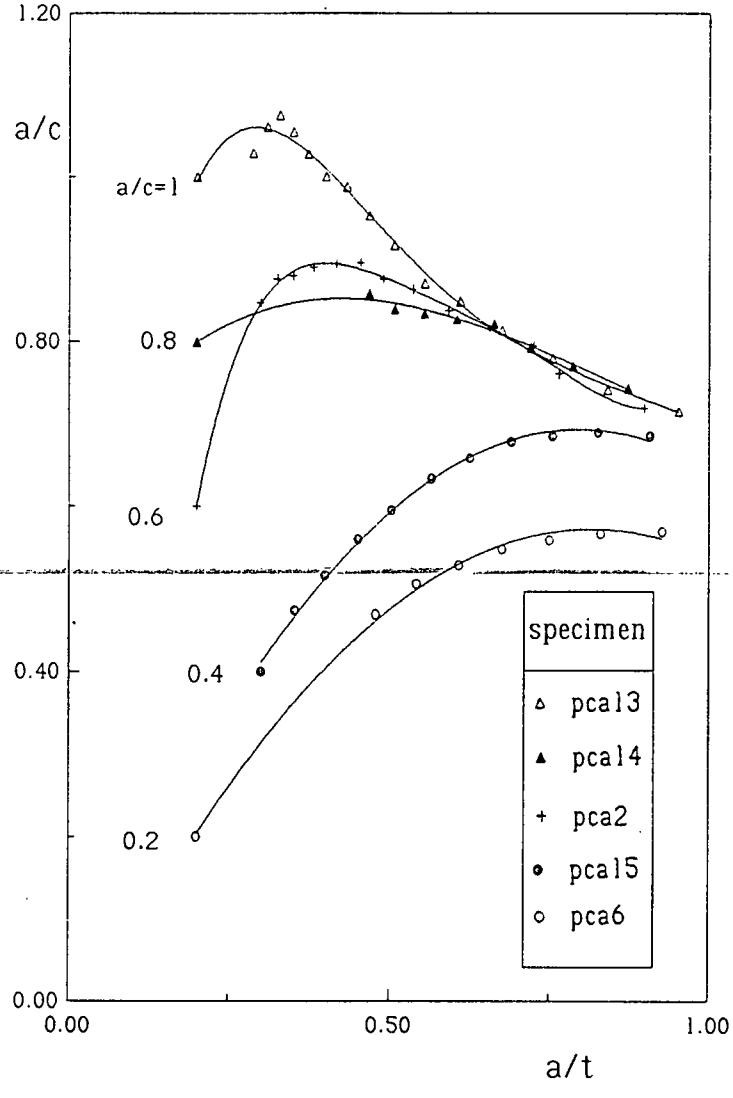

Figure 14. Crack shape development curves of different initial aspect ratio (a/c).

APPENDIX 1 COMPILATION OF EXPERIMENTAL DATA

In this appendix information on S_{op} measurement results is given. The crack front numbering is shown in figure A1. Number 1 is the last one before breakthrough. Due to difficulties in the measurement of S_{op} the last crack front at or before breakthrough was not included. For the same reason, points on the specimen surface were not included. The x and y coordinates correspond to coordinates of the fitted ellipses and increment of the angle(ϕ) (figure 3) of 15°. ΔK was determined with the Newman-Raju solution (Appendix 2), while ΔK_{eff} was calculated by replacing S in the Newman-Raju solution with $(S_{max} - S_{op})$.

The S_{op}-value was obtained as a result of our fractographic measurements. Calculated da/dn values were obtained from through crack data (C = 2.29*E-04, m = 2.88 for ΔK and C = 4.36*E-04, m = 2.88 for ΔK_{eff}) with K in MPa m and da/dn in mm/kc.

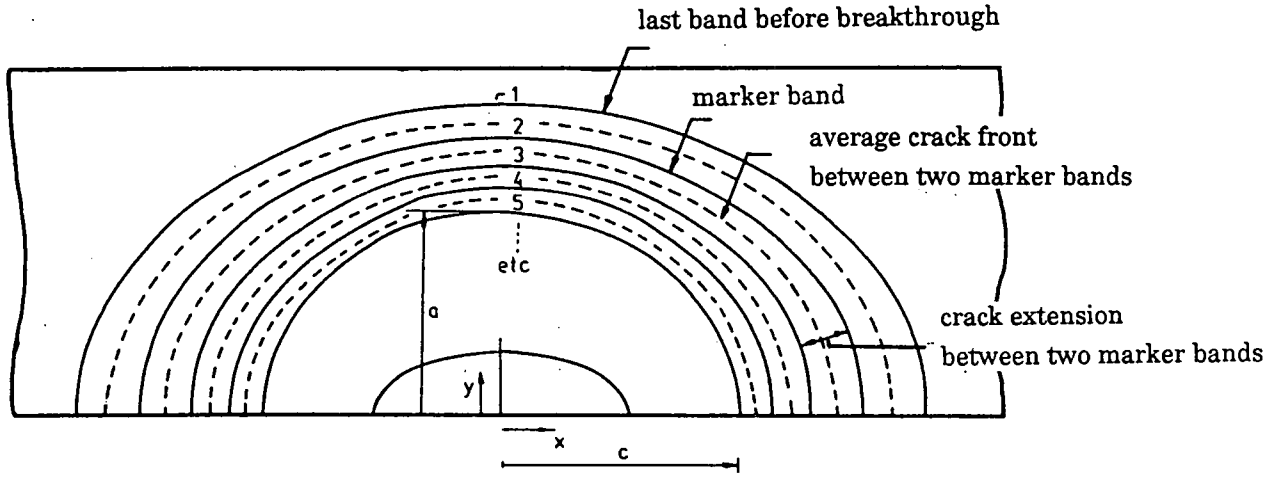

Figure A-1. Crack front marker-band numbering and related notations (for definition of angle ϕ see figure 3).

Specimen : PCA2 Crack front no: 1											
No	Coordinate		Elliptical parameter			ΔK $MPa\sqrt{m}$	S_{op} MPa	ΔK_{eff} $MPa\sqrt{m}$	da/dn (mm/kc)		
	x	y	a	c	ϕ				test	based on ΔK	based on ΔK_{eff}
1	10.69	2.12	8.18	11.07	15	20.93	27.0	19.07	1.71	1.46	2.12
2	9.59	4.09	8.18	11.07	30	19.72	25.5	18.19	1.48	1.23	1.85
3	7.83	5.78	8.18	11.07	45	19.42	24.0	18.13	1.24	1.17	1.83
4	5.54	7.08	8.18	11.07	60	19.63	24.0	18.32	1.05	1.21	1.89
5	2.86	7.90	8.18	11.07	75	19.96	22.5	18.85	0.93	1.27	2.05
6	0.00	8.18	8.18	11.07	90	20.10	22.5	18.99	0.89	1.30	2.10

Specimen : PCA2 Crack front no: 2											
No	Coordinate		Elliptical parameter			ΔK $MPa\sqrt{m}$	S_{op}	ΔK_{eff} $MPa\sqrt{m}$	da/dn (mm/kc)		
	x	y	a	c	ϕ				test	based on ΔK	based on ΔK_{eff}
1	9.13	1.90	7.34	9.45	15	18.69	28.5	16.82	1.35	1.05	1.48
2	8.18	3.67	7.34	9.45	30	17.71	27.0	16.14	1.20	0.90	1.31
3	6.68	5.19	7.34	9.45	45	17.45	28.5	15.71	1.64	0.86	1.21
4	4.72	6.36	7.34	9.45	60	17.61	28.5	15.85	0.90	0.89	1.25
5	2.45	7.09	7.34	9.45	75	17.86	25.5	16.47	0.81	0.92	1.39
6	0.00	7.34	7.34	9.45	90	17.97	24.0	16.78	0.79	0.94	1.47

Specimen : PCA2 Crack front no: 3											
	Coordinate		Elliptical parameter			ΔK $MPa\sqrt{m}$	S_{op}	ΔK_{eff} $MPa\sqrt{m}$	da/dn (mm/kc)		
No	x	y	a	c	ϕ				test	based on ΔK	based on ΔK_{eff}
1	7.94	1.71	6.61	8.22	15	16.93	30.0	15.05	1.02	0.79	1.07
2	7.12	3.30	6.61	8.22	30	16.12	27.0	14.69	0.93	0.69	1.00
3	5.81	4.67	6.61	8.22	45	15.91	23.5	14.91	0.83	0.66	1.04
4	4.11	5.72	6.61	8.22	60	16.03	27.0	14.61	0.75	0.68	0.98
5	2.13	6.38	6.61	8.22	75	16.24	29.2	14.52	0.69	0.70	0.96
6	0.00	6.61	6.61	8.22	90	16.33	26.2	14.97	0.67	0.71	1.05

Specimen : PCA2 Crack front no: 4											
	Coordinate		Elliptical parameter			ΔK $MPa\sqrt{m}$	S_{op}	ΔK_{eff} $MPa\sqrt{m}$	da/dn (mm/kc)		
No	x	y	a	c	ϕ				test	based on ΔK	based on ΔK_{eff}
1	6.97	1.54	5.97	7.22	15	15.49	28.5	13.94	0.90	0.61	0.86
2	6.25	2.98	5.97	7.22	30	14.81	27.0	13.49	0.83	0.54	0.78
3	5.10	4.22	5.97	7.22	45	14.63	26.2	13.41	0.75	0.52	0.77
4	3.61	5.17	5.97	7.22	60	14.73	28.5	13.25	0.67	0.53	0.74
5	1.87	5.77	5.97	7.22	75	14.89	30.8	13.15	0.63	0.55	0.73
6	0.00	5.97	5.97	7.22	90	14.97	27.8	13.55	0.61	0.56	0.79

Specimen : PCA2 Crack front no: 5											
	Coordinate		Elliptical parameter						da/dn (mm/kc)		
No	x	y	a	c	ϕ	ΔK $MPa\sqrt{m}$	S_{op}	ΔK_{eff} $MPa\sqrt{m}$	test	based on ΔK	based on ΔK_{eff}
1	6.13	1.40	5.40	6.35	15	14.26	32.0	12.46	0.79	0.48	0.62
2	5.50	2.70	5.40	6.35	30	13.68	32.0	11.95	0.73	0.43	0.55
3	4.49	3.82	5.40	6.35	45	13.51	31.5	11.86	0.65	0.41	0.54
4	3.18	4.68	5.40	6.35	60	13.58	28.5	12.22	0.59	0.42	0.59
5	1.64	5.22	5.40	6.35	75	13.71	30.0	12.19	0.54	0.43	0.58
6	0.00	5.40	5.40	6.35	90	13.77	25.5	12.70	0.53	0.44	0.65

Specimen : PCA2 Crack front no: 6											
	Coordinate		Elliptical parameter						da/dn (mm/kc)		
No	x	y	a	c	ϕ	ΔK $MPa\sqrt{m}$	S_{op}	ΔK_{eff} $MPa\sqrt{m}$	test	based on ΔK	based on ΔK_{eff}
1	5.46	1.27	4.91	5.65	15	13.26	31.5	11.64	0.58	0.39	0.51
2	4.89	2.46	4.91	5.65	30	12.75	31.5	11.19	0.55	0.35	0.46
3	4.00	3.47	4.91	5.65	45	12.59	27.8	11.40	0.51	0.34	0.48
4	2.82	4.25	4.91	5.65	60	12.64	28.5	11.38	0.48	0.34	0.48
5	1.46	4.74	4.91	5.65	75	12.75	25.5	11.76	0.45	0.35	0.53
6	0.00	4.91	4.91	5.65	90	12.80	25.5	11.80	0.44	0.35	0.53

Specimen : PCA2 Crack front no: 7											
	Coordinate		Elliptical parameter						da/dn (mm/kc)		
No	x	y	a	c	ϕ	ΔK $MPa\sqrt{m}$	S_{op}	ΔK_{eff} $MPa\sqrt{m}$	test	based on ΔK	based on ΔK_{eff}
1	4.93	1.17	4.52	5.10	15	12.48	30.0	11.09	0.49	0.33	0.44
2	4.42	2.26	4.52	5.10	30	12.01	28.5	10.81	0.46	0.29	0.41
3	3.61	3.20	4.52	5.10	45	11.86	26.2	10.87	0.42	0.28	0.42
4	2.55	3.91	4.52	5.10	60	11.89	25.5	10.97	0.38	0.28	0.43
5	1.32	4.37	4.52	5.10	75	11.98	24.0	11.18	0.36	0.29	0.46
6	0.00	4.52	4.52	5.10	90	12.02	24.0	11.22	0.35	0.30	0.46

Specimen : PCA2 Crack front no: 8											
	Coordinate		Elliptical parameter						da/dn (mm/kc)		
No	x	y	a	c	ϕ	ΔK $MPa\sqrt{m}$	S_{op}	ΔK_{eff} $MPa\sqrt{m}$	test	based on ΔK	based on ΔK_{eff}
1	4.49	1.08	4.17	4.65	15	11.80	27.0	10.76	0.39	0.28	0.41
2	4.03	2.08	4.17	4.65	30	11.39	25.5	10.50	0.38	0.25	0.38
3	3.29	2.95	4.17	4.65	45	11.25	24.0	10.50	0.37	0.24	0.38
4	2.32	3.61	4.17	4.65	60	11.27	22.5	10.64	0.36	0.24	0.40
5	1.20	4.03	4.17	4.65	75	11.34	22.5	10.71	0.36	0.25	0.40
6	0.00	4.17	4.17	4.65	90	11.38	22.5	10.74	0.36	0.25	0.41

Specimen : PCA2 Crack front no: 9											
	Coordinate		Elliptical parameter			ΔK $MPa\sqrt{m}$	S_{op}	ΔK_{eff} $MPa\sqrt{m}$	da/dn (mm/kc)		
No	x	y	a	c	ϕ				test	based on ΔK	based on ΔK_{eff}
1	4.13	0.99	3.82	4.28	15	11.17	25.5	10.30	0.35	0.24	0.36
2	3.71	1.91	3.82	4.28	30	10.81	25.5	9.97	0.35	0.22	0.33
3	3.03	2.70	3.82	4.28	45	10.70	22.5	10.11	0.34	0.21	0.34
4	2.14	3.31	3.82	4.28	60	10.74	22.5	10.14	0.34	0.21	0.34
5	1.11	3.69	3.82	4.28	75	10.81	22.5	10.21	0.34	0.22	0.35
6	0.00	3.82	3.82	4.28	90	10.84	22.5	10.25	0.34	0.22	0.36

Specimen : PCA2 Crack front no: 10											
	Coordinate		Elliptical parameter			ΔK $MPa\sqrt{m}$	S_{op}	ΔK_{eff} $MPa\sqrt{m}$	da/dn (mm/kc)		
No	x	y	a	c	ϕ				test	based on ΔK	based on ΔK_{eff}
1	3.82	0.91	3.50	3.95	15	10.59	24.0	9.89	0.30	0.20	0.32
2	3.42	1.75	3.50	3.95	30	10.29	24.0	9.60	0.30	0.19	0.29
3	2.79	2.47	3.50	3.95	45	10.21	22.5	9.64	0.30	0.18	0.30
4	1.98	3.03	3.50	3.95	60	10.25	21.0	9.80	0.30	0.19	0.31
5	1.02	3.38	3.50	3.95	75	10.33	21.0	9.87	0.30	0.19	0.32
6	0.00	3.50	3.50	3.95	90	10.37	21.0	9.91	0.30	0.19	0.32

Specimen : PCA2 Crack front no: 11											
	Coordinate		Elliptical parameter						da/dn (mm/kc)		
No	x	y	a	c	ϕ	ΔK $MPa\sqrt{m}$	S_{op}	ΔK_{eff} $MPa\sqrt{m}$	test	based on ΔK	based on ΔK_{eff}
1	3.55	0.84	3.23	3.68	15	10.11	21.0	9.66	0.25	0.18	0.30
2	3.19	1.62	3.23	3.68	30	9.84	21.0	9.40	0.25	0.17	0.28
3	2.60	2.28	3.23	3.68	45	9.79	21.0	9.35	0.24	0.16	0.27
4	1.84	2.80	3.23	3.68	60	9.85	19.5	9.52	0.24	0.17	0.29
5	0.95	3.11	3.23	3.68	75	9.93	19.5	9.60	0.24	0.17	0.29
6	0.00	3.23	3.23	3.68	90	9.87	19.5	9.64	0.24	0.17	0.29

Specimen : PCA2 Crack front no: 12											
	Coordinate		Elliptical parameter						da/dn (mm/kc)		
No	x	y	a	c	ϕ	ΔK $MPa\sqrt{m}$	S_{op}	ΔK_{eff} $MPa\sqrt{m}$	test	based on ΔK	based on ΔK_{eff}
1	3.35	0.77	2.99	3.47	15	9.68	15.0	9.68	0.18	0.16	0.16
2	3.01	1.50	2.99	3.47	30	9.46	15.0	9.46	0.19	0.15	0.15
3	2.45	2.11	2.99	3.47	45	9.44	15.0	9.44	0.21	0.15	0.15
4	1.74	2.59	2.99	3.47	60	9.52	15.0	9.52	0.23	0.15	0.15
5	0.90	2.89	2.99	3.47	75	9.62	15.0	9.62	0.24	0.16	0.16
6	0.00	2.99	2.99	3.47	90	9.66	15.0	9.66	0.25	0.16	0.16

Specimen : PCA6 Crack front no: 1											
	Coordinate		Elliptical parameter			ΔK $MPa\sqrt{m}$	S_{op}	ΔK_{eff} $MPa\sqrt{m}$	da/dn (mm/kc)		
No	x	y	a	c	ϕ				test	based on ΔK	based on ΔK_{eff}
1	13.03	1.95	7.53	13.49	15	21.05	37.5	17.54	1.65	1.48	1.67
2	11.68	3.76	7.53	13.49	30	20.87	37.5	17.39	1.49	1.44	1.63
3	9.54	5.32	7.53	13.49	45	21.44	37.5	17.87	1.37	1.56	1.76
4	6.74	6.52	7.53	13.49	60	22.25	34.5	19.04	1.30	1.74	2.11
5	3.49	7.27	7.53	13.49	75	22.93	34.5	19.62	1.26	1.90	2.30
6	0.00	7.53	7.53	13.49	90	23.20	34.5	20.36	1.25	1.96	2.56

Specimen : PCA6 Crack front no: 2											
	Coordinate		Elliptical parameter			ΔK $MPa\sqrt{m}$	S_{op}	ΔK_{eff} $MPa\sqrt{m}$	da/dn (mm/kc)		
No	x	y	a	c	ϕ				test	based on ΔK	based on ΔK_{eff}
1	12.00	1.64	6.35	12.42	15	18.11	36.0	15.29	1.31	0.96	1.12
2	10.76	3.18	6.35	12.42	30	18.50	34.5	15.83	1.20	1.02	1.24
3	8.78	4.49	6.35	12.42	45	19.39	33.0	16.80	1.14	1.17	1.47
4	6.21	5.50	6.35	12.42	60	20.33	37.5	16.94	1.11	1.34	1.51
5	3.21	6.13	6.35	12.42	75	21.03	34.5	17.99	1.10	1.48	1.79
6	0.00	6.35	6.35	12.42	90	21.29	31.5	18.69	1.09	1.53	2.00

Specimen : PCA6 Crack front no: 3											
	Coordinate		Elliptical parameter			ΔK $MPa\sqrt{m}$	S_{op}	ΔK_{eff} $MPa\sqrt{m}$	da/dn (mm/kc)		
No	x	y	a	c	ϕ				test	based on ΔK	based on ΔK_{eff}
1	10.35	1.37	5.29	10.72	15	15.34	30.0	13.63	0.99	0.60	0.81
2	9.28	2.64	5.29	10.72	30	15.95	33.0	13.82	0.96	0.67	0.84
3	7.58	3.74	5.29	10.72	45	16.90	31.5	14.84	0.97	0.79	1.03
4	5.36	4.58	5.29	10.72	60	17.82	36.0	15.04	1.00	0.92	1.07
5	2.77	5.11	5.29	10.72	75	18.47	33.0	16.00	1.02	1.02	1.28
6	0.00	5.29	5.29	10.72	90	18.70	31.5	16.42	1.03	1.05	1.38

Specimen : PCA6 Crack front no: 4											
	Coordinate		Elliptical parameter			ΔK $MPa\sqrt{m}$	S_{op}	ΔK_{eff} $MPa\sqrt{m}$	da/dn (mm/kc)		
No	x	y	a	c	ϕ				test	based on ΔK	based on ΔK_{eff}
1	9.67	1.12	4.32	10.01	15	13.03	25.5	12.02	0.45	0.37	0.56
2	8.67	2.16	4.32	10.01	30	14.01	33.0	12.14	0.58	0.46	0.58
3	7.08	3.05	4.32	10.01	45	15.14	28.5	13.63	0.71	0.57	0.81
4	5.00	3.74	4.32	10.01	60	16.12	30.0	14.33	0.82	0.69	0.93
5	2.59	4.17	4.32	10.01	75	16.77	31.5	14.72	0.89	0.77	1.01
6	0.00	4.32	4.32	10.01	90	17.01	30.0	15.12	0.92	0.80	1.09

Specimen : PCA6 Crack front no: 5											
	Coordinate		Elliptical parameter			ΔK $MPa\sqrt{m}$	S_{op}	ΔK_{eff} $MPa\sqrt{m}$	da/dn (mm/kc)		
No	x	y	a	c	ϕ				test	based on ΔK	based on ΔK_{eff}
1	9.30	0.90	3.48	9.63	15	11.02	-	-	-	-	-
2	8.34	1.74	3.48	9.63	30	12.32	28.5	11.08	0.49	0.32	0.44
3	6.81	2.46	3.48	9.63	45	13.58	27.0	12.38	0.59	0.42	0.61
4	4.82	3.01	3.48	9.63	60	14.59	27.0	13.29	0.68	0.52	0.75
5	2.49	3.36	3.48	9.63	75	15.24	27.0	13.89	0.74	0.58	0.85
6	0.00	3.48	3.48	9.63	90	15.47	27.0	14.10	0.76	0.61	0.89

Specimen : PCA6 Crack front no: 6											
	Coordinate		Elliptical parameter			ΔK $MPa\sqrt{m}$	S_{op}	ΔK_{eff} $MPa\sqrt{m}$	da/dn (mm/kc)		
No	x	y	a	c	ϕ				test	based on ΔK	based on ΔK_{eff}
1	8.86	0.73	2.82	9.18	15	-	-	-	-	-	-
2	7.95	1.41	2.82	9.18	30	-	-	-	-	-	-
3	6.49	1.99	2.82	9.18	45	-	-	-	-	-	-
4	4.59	2.44	2.82	9.18	60	13.15	25.5	12.13	0.53	0.38	0.58
5	2.38	2.72	2.82	9.18	75	13.78	25.5	12.70	0.55	0.44	0.66
6	0.00	2.82	2.82	9.18	90	13.99	24.0	13.06	0.56	0.46	0.71

Specimen : PCA13 Crack front no: 1											
	Coordinate		Elliptical parameter			ΔK $MPa\sqrt{m}$	S_{op}	ΔK_{eff} $MPa\sqrt{m}$	da/dn (mm/kc)		
No	x	y	a	c	ϕ				test	based on ΔK	based on ΔK_{eff}
1	11.43	2.23	8.61	11.83	15	22.05	28.5	19.84	1.82	1.69	2.38
2	10.24	4.30	8.61	11.83	30	20.69	25.5	19.08	1.61	1.41	2.12
3	8.36	6.09	8.61	11.83	45	20.34	25.5	18.76	1.40	1.34	2.02
4	5.92	7.46	8.61	11.83	60	20.55	25.5	18.95	1.22	1.38	2.08
5	3.06	8.32	8.61	11.83	75	20.90	21.0	19.97	1.12	1.45	2.42
6	0.00	8.61	8.61	11.83	90	21.06	21.0	21.12	1.08	1.48	2.48

Specimen : PCA13 Crack front no: 2											
	Coordinate		Elliptical parameter			ΔK $MPa\sqrt{m}$	S_{op}	ΔK_{eff} $MPa\sqrt{m}$	da/dn (mm/kc)		
No	x	y	a	c	ϕ				test	based on ΔK	based on ΔK_{eff}
1	9.73	1.98	7.65	10.07	15	19.52	30.0	17.35	1.52	1.19	1.62
2	8.72	3.82	7.65	10.07	30	18.47	28.5	16.62	1.33	1.02	1.43
3	7.12	5.41	7.65	10.07	45	18.21	27.0	16.59	1.13	0.98	1.42
4	5.04	6.62	7.65	10.07	60	18.39	27.0	16.76	0.97	1.00	1.46
5	2.61	7.39	7.65	10.07	75	18.67	23.0	17.57	0.87	1.05	1.68
6	0.00	7.65	7.65	10.07	90	18.80	23.0	17.69	0.83	1.07	1.71

Specimen : PCA13 Crack front no: 3											
	Coordinate		Elliptical parameter			ΔK $MPa\sqrt{m}$	S_{op}	ΔK_{eff} $MPa\sqrt{m}$	da/dn (mm/kc)		
No	x	y	a	c	ϕ				test	based on ΔK	based on ΔK_{eff}
1	8.32	1.77	6.85	8.61	15	17.50	31.5	15.36	1.27	0.87	1.14
2	7.46	3.42	6.85	8.61	30	16.63	28.5	14.97	1.14	0.75	1.06
3	6.09	4.84	6.85	8.61	45	16.40	27.0	14.94	1.00	0.72	1.05
4	4.30	5.93	6.85	8.61	60	16.53	30.0	14.70	0.87	0.74	1.00
5	2.23	6.62	6.85	8.61	75	16.75	28.5	15.08	0.79	0.77	1.08
6	0.00	6.85	6.85	8.61	90	16.85	28.5	15.17	0.76	0.78	1.10

Specimen : PCA13 Crack front no: 4											
	Coordinate		Elliptical parameter			ΔK $MPa\sqrt{m}$	S_{op}	ΔK_{eff} $MPa\sqrt{m}$	da/dn (mm/kc)		
No	x	y	a	c	ϕ				test	based on ΔK	based on ΔK_{eff}
1	7.17	1.59	6.16	7.42	15	15.86	31.5	13.92	1.02	0.66	0.86
2	6.43	3.08	6.16	7.42	30	15.13	28.5	13.61	0.93	0.57	0.80
3	5.25	4.36	6.16	7.42	45	14.91	25.5	13.75	0.81	0.55	0.83
4	3.71	5.33	6.16	7.42	60	15.00	27.0	13.66	0.71	0.56	0.81
5	1.92	5.95	6.16	7.42	75	15.16	28.5	13.64	0.64	0.58	0.81
6	0.00	6.16	6.16	7.42	90	15.23	28.5	13.71	0.62	0.58	0.82

Specimen : PCA13 Crack front no: 5											
	Coordinate		Elliptical parameter						da/dn (mm/kc)		
No	x	y	a	c	ϕ	ΔK $MPa\sqrt{m}$	S_{op}	ΔK_{eff} $MPa\sqrt{m}$	test	based on ΔK	based on ΔK_{eff}
1	6.24	1.44	5.58	6.46	15	14.56	34.5	12.45	0.81	0.51	0.62
2	5.59	2.79	5.58	6.46	30	13.91	31.5	12.21	0.75	0.45	0.59
3	4.57	3.95	5.58	6.46	45	13.70	30.0	12.17	0.67	0.43	0.58
4	3.23	4.83	5.58	6.46	60	13.74	27.0	12.52	0.60	0.43	0.63
5	1.67	5.39	5.58	6.46	75	13.85	25.5	12.78	0.56	0.44	0.67
6	0.00	5.58	5.58	6.46	90	13.91	25.5	12.83	0.54	0.45	0.68

Specimen : PCA13 Crack front no: 6											
	Coordinate		Elliptical parameter						da/dn (mm/kc)		
No	x	y	a	c	ϕ	ΔK $MPa\sqrt{m}$	S_{op}	ΔK_{eff} $MPa\sqrt{m}$	test	based on ΔK	based on ΔK_{eff}
1	5.47	1.31	5.08	5.66	15	13.48	34.5	11.53	0.73	0.41	0.50
2	4.90	2.54	5.08	5.66	30	12.90	31.5	11.32	0.67	0.36	0.47
3	4.00	3.59	5.08	5.66	45	12.68	31.5	11.13	0.59	0.34	0.45
4	2.83	4.40	5.08	5.66	60	12.67	28.5	11.41	0.52	0.34	0.48
5	1.46	4.91	5.08	5.66	75	12.74	25.5	11.76	0.47	0.35	0.53
6	0.00	5.08	5.08	5.66	90	12.79	25.5	11.79	0.45	0.35	0.53

Specimen : PCA13 Crack front no: 7											
	Coordinate		Elliptical parameter			ΔK $MPa\sqrt{m}$	S_{op}	ΔK_{eff} $MPa\sqrt{m}$	da/dn (mm/kc)		
No	x	y	a	c	ϕ				test	based on ΔK	based on ΔK_{eff}
1	4.83	1.21	4.67	5.00	15	12.62	30.0	11.22	0.57	0.34	0.46
2	4.33	2.34	4.67	5.00	30	12.07	28.5	10.86	0.52	0.30	0.42
3	3.54	3.30	4.67	5.00	45	11.83	27.0	10.78	0.47	0.28	0.41
4	2.50	4.04	4.67	5.00	60	11.78	24.0	11.00	0.42	0.28	0.44
5	1.29	4.51	4.67	5.00	75	11.81	24.0	11.02	0.38	0.28	0.44
6	0.00	4.67	4.67	5.00	90	11.84	22.5	11.18	0.36	0.28	0.46

Specimen : PCA13 Crack front no: 8											
	Coordinate		Elliptical parameter			ΔK $MPa\sqrt{m}$	S_{op}	ΔK_{eff} $MPa\sqrt{m}$	da/dn (mm/kc)		
No	x	y	a	c	ϕ				test	based on ΔK	based on ΔK_{eff}
1	4.30	1.12	4.32	4.45	15	11.90	30.0	10.57	0.50	0.29	0.39
2	3.85	2.16	4.32	4.45	30	11.37	28.5	10.23	0.47	0.25	0.35
3	3.15	3.05	4.32	4.45	45	11.11	25.5	10.24	0.42	0.24	0.35
4	2.22	3.74	4.32	4.45	60	11.02	24.0	10.28	0.38	0.23	0.36
5	1.15	4.17	4.32	4.45	75	11.02	22.5	10.41	0.35	0.23	0.37
6	0.00	4.32	4.32	4.45	90	11.03	22.5	10.41	0.34	0.22	0.37

Specimen : PCA13 Crack front no: 9											
	Coordinate		Elliptical parameter						da/dn (mm/kc)		
No	x	y	a	c	ϕ	ΔK $MPa\sqrt{m}$	S_{op}	ΔK_{eff} $MPa\sqrt{m}$	test	based on ΔK	based on ΔK_{eff}
1	3.88	1.03	3.99	4.02	15	11.30	28.5	10.17	0.35	0.25	0.34
2	3.48	2.00	3.99	4.02	30	10.81	27.0	9.85	0.34	0.22	0.32
3	2.84	2.82	3.99	4.02	45	10.54	25.5	9.72	0.33	0.20	0.30
4	2.01	3.46	3.99	4.02	60	10.44	25.5	9.62	0.32	0.20	0.30
5	1.04	3.85	3.99	4.02	75	10.42	22.5	9.84	0.31	0.20	0.32
6	0.00	3.99	3.99	4.02	90	10.42	22.5	9.84	0.31	0.19	0.32

Specimen : PCA13 Crack front no: 10											
	Coordinate		Elliptical parameter						da/dn (mm/kc)		
No	x	y	a	c	ϕ	ΔK $MPa\sqrt{m}$	S_{op}	ΔK_{eff} $MPa\sqrt{m}$	test	based on ΔK	based on ΔK_{eff}
1	3.54	0.96	3.71	3.66	15	10.66	25.5	9.83	0.35	0.21	0.32
2	3.17	1.86	3.71	3.66	30	10.20	25.5	9.40	0.33	0.18	0.28
3	2.59	2.62	3.71	3.66	45	9.94	25.5	9.16	0.31	0.17	0.26
4	1.83	3.21	3.71	3.66	60	9.82	22.5	9.27	0.28	0.16	0.27
5	0.95	3.58	3.71	3.66	75	9.78	22.5	9.24	0.27	0.16	0.26
6	0.00	3.71	3.71	3.66	90	9.77	22.5	9.23	0.26	0.16	0.26

Specimen : PCA13 Crack front no: 11											
	Coordinate		Elliptical parameter						da/dn (mm/kc)		
No	x	y	a	c	ϕ	ΔK $MPa\sqrt{m}$	S_{op}	ΔK_{eff} $MPa\sqrt{m}$	test	based on ΔK	based on ΔK_{eff}
1	3.22	0.90	3.46	3.33	15	10.06	25.5	9.27	0.30	0.18	0.27
2	2.88	1.73	3.46	3.33	30	9.62	22.5	9.08	0.28	0.16	0.25
3	2.35	2.45	3.46	3.33	45	9.36	22.5	8.84	0.26	0.14	0.23
4	1.67	3.00	3.46	3.33	60	9.22	22.5	8.71	0.24	0.14	0.22
5	0.86	3.34	3.46	3.33	75	9.17	22.5	8.66	0.23	0.14	0.22
6	0.00	3.46	3.46	3.33	90	9.15	22.5	8.64	0.22	0.13	0.22

Specimen : PCA13 Crack front no: 12											
	Coordinate		Elliptical parameter						da/dn (mm/kc)		
No	x	y	a	c	ϕ	ΔK $MPa\sqrt{m}$	S_{op}	ΔK_{eff} $MPa\sqrt{m}$	test	based on ΔK	based on ΔK_{eff}
1	2.96	0.84	3.25	3.06	15	9.56	25.5	8.82	0.24	0.15	0.23
2	2.65	1.62	3.25	3.06	30	9.14	22.5	8.64	0.24	0.13	0.22
3	2.16	2.30	3.25	3.06	45	8.88	22.5	8.38	0.22	0.12	0.20
4	1.53	2.81	3.25	3.06	60	8.73	21.0	8.34	0.21	0.12	0.20
5	0.79	3.14	3.25	3.06	75	8.66	21.0	8.27	0.20	0.11	0.19
6	0.00	3.25	3.25	3.06	90	8.64	21.0	8.25	0.20	0.11	0.19

Specimen : PCA13 Crack front no: 13											
	Coordinate		Elliptical parameter						da/dn (mm/kc)		
No	x	y	a	c	ϕ	ΔK $MPa\sqrt{m}$	S_{op}	ΔK_{eff} $MPa\sqrt{m}$	test	based on ΔK	based on ΔK_{eff}
1	2.76	0.79	3.06	2.86	15	9.19	22.5	8.68	0.14	0.14	0.22
2	2.48	1.53	3.06	2.86	30	8.80	22.5	8.31	0.15	0.12	0.19
3	2.02	2.16	3.06	2.86	45	8.54	19.5	8.26	0.16	0.11	0.19
4	1.43	2.65	3.06	2.86	60	8.39	19.5	8.11	0.18	0.10	0.18
5	0.74	2.96	3.06	2.86	75	8.32	19.5	8.04	0.18	0.10	0.17
6	0.00	3.06	3.06	2.86	90	8.30	19.5	8.02	0.19	0.10	0.18

Specimen : PCA14 Crack front no: 1											
	Coordinate		Elliptical parameter						da/dn (mm/kc)		
No	x	y	a	c	ϕ	ΔK $MPa\sqrt{m}$	S_{op}	$\Delta Keff$ $MPa\sqrt{m}$	test	based on ΔK	based on $\Delta Keff$
1	10.18	2.06	7.97	10.54	15	20.28	33.0	17.58	1.41		
2	9.13	3.98	7.97	10.54	30	19.12	31.5	16.78	1.26		
3	7.45	5.64	7.97	10.54	45	18.81	28.5	16.92	1.09		
4	5.27	6.90	7.97	10.54	60	18.98	28.5	17.08	0.95		
5	2.73	7.70	7.97	10.54	75	19.27	28.5	17.34	0.87		
6	0.00	7.97	7.97	10.54	90	19.40	27.0	17.68	0.84		

Specimen : PCA14 Crack front no: 2											
	Coordinate		Elliptical parameter						da/dn (mm/kc)		
No	x	y	a	c	ϕ	ΔK $MPa\sqrt{m}$	S_{op}	$\Delta Keff$ $MPa\sqrt{m}$	test	based on ΔK	based on $\Delta Keff$
1	8.94	1.87	7.23	9.26	15	18.42	34.5	15.76	1.05	1.01	1.22
2	8.02	3.62	7.23	9.26	30	17.47	36.0	14.75	0.94	0.87	1.01
3	6.55	5.11	7.23	9.26	45	17.22	33.0	14.92	0.82	0.83	1.05
4	4.63	6.26	7.23	9.26	60	17.37	31.5	15.24	0.72	0.85	1.11
5	2.40	6.98	7.23	9.26	75	17.61	31.5	15.46	0.66	0.89	1.16
6	0.00	7.23	7.23	9.26	90	17.72	30.0	15.75	0.64	0.90	1.22

Specimen : PCA14 Crack front no: 3											
	Coordinate		Elliptical parameter						da/dn (mm/kc)		
No	x	y	a	c	ϕ	ΔK $MPa\sqrt{m}$	S_{op}	$\Delta Keff$ $MPa\sqrt{m}$	test	based on ΔK	based on $\Delta Keff$
1	7.94	1.72	6.63	8.22	15	17.49	36.0	14.32	0.94	0.87	0.93
2	7.12	3.32	6.63	8.22	30	16.90	37.5	13.45	0.85	0.79	0.78
3	5.81	4.69	6.63	8.22	45	16.93	34.5	13.62	0.74	0.79	0.80
4	4.11	5.74	6.63	8.22	60	17.26	33.0	13.90	0.64	0.84	0.85
5	2.12	6.40	6.63	8.22	75	17.60	31.5	14.25	0.58	0.88	0.92
6	0.00	6.63	6.63	8.22	90	17.75	31.5	14.33	0.56	0.91	0.93

Specimen : PCA14 Crack front no: 4											
	Coordinate		Elliptical parameter						da/dn (mm/kc)		
No	x	y	a	c	ϕ	ΔK $MPa\sqrt{m}$	S_{op}	$\Delta Keff$ $MPa\sqrt{m}$	test	based on ΔK	based on $\Delta Keff$
1	7.11	1.57	6.07	7.36	15	15.70	37.5	13.08	0.71	0.64	0.72
2	6.37	3.04	6.07	7.36	30	15.00	36.0	12.67	0.67	0.56	0.65
3	5.20	4.29	6.07	7.36	45	14.81	34.5	12.67	0.63	0.54	0.64
4	3.68	5.26	6.07	7.36	60	14.91	36.0	12.59	0.59	0.55	0.64
5	1.90	5.86	6.07	7.36	75	15.08	33.0	13.07	0.56	0.57	0.72
6	0.00	6.07	6.07	7.36	90	15.16	33.0	13.14	0.56	0.58	0.73

Specimen : PCA14 Crack front no: 5											
	Coordinate		Elliptical parameter						da/dn (mm/kc)		
No	x	y	a	c	ϕ	ΔK $MPa\sqrt{m}$	S_{op}	$\Delta Keff$ $MPa\sqrt{m}$	test	based on ΔK	based on $\Delta Keff$
1	6.45	1.44	5.55	6.68	15	14.63	40.5	11.86	0.63	0.52	0.54
2	5.78	2.78	5.55	6.68	30	14.04	39.0	11.55	0.60	0.46	0.50
3	4.72	3.92	5.55	6.68	45	13.90	37.5	11.58	0.56	0.45	0.50
4	3.34	4.81	5.55	6.68	60	14.00	37.5	11.67	0.52	0.46	0.52
5	1.73	5.36	5.55	6.68	75	14.16	36.0	11.96	0.50	0.47	0.55
6	0.00	5.55	5.55	6.68	90	14.23	34.5	12.18	0.49	0.48	0.58

Specimen : PCA14 Crack front no: 6											
	Coordinate		Elliptical parameter						da/dn (mm/kc)		
No	x	y	a	c	ϕ	ΔK $MPa\sqrt{m}$	S_{op}	$\Delta Keff$ $MPa\sqrt{m}$	test	based on ΔK	based on $\Delta Keff$
1	5.86	1.32	5.09	6.07	15	13.94	43.5	10.80	0.56	0.45	0.41
2	5.26	2.54	5.09	6.07	30	13.60	42.0	10.56	0.53	0.42	0.39
3	4.29	3.60	5.09	6.07	45	13.65	39.0	10.76	0.50	0.42	0.41
4	3.04	4.41	5.09	6.07	60	13.90	37.5	10.99	0.47	0.45	0.43
5	1.57	4.92	5.09	6.07	75	14.14	37.5	11.11	0.45	0.50	0.45
6	0.00	5.09	5.09	6.07	90	14.24	36.0	11.31	0.44	0.48	0.47

Specimen : PCA14 Crack front no: 7											
	Coordinate		Elliptical parameter						da/dn (mm/kc)		
No	x	y	a	c	ϕ	ΔK $MPa\sqrt{m}$	S_{op}	$\Delta Keff$ $MPa\sqrt{m}$	test	based on ΔK	based on $\Delta Keff$
1	5.31	1.21	4.67	5.50	15	12.86	42.0	10.29	0.55	0.36	0.36
2	4.76	2.34	4.67	5.50	30	12.42	40.5	10.08	0.51	0.32	0.38
3	3.89	3.30	4.67	5.50	45	12.32	39.0	10.13	0.47	0.32	0.34
4	2.75	4.04	4.67	5.50	60	12.41	37.5	10.34	0.42	0.32	0.36
5	1.42	4.51	4.67	5.50	75	12.54	36.0	10.59	0.40	0.33	0.39
6	0.00	4.67	4.67	5.50	90	12.60	36.0	10.64	0.38	0.34	0.40

Specimen : PCA15 Crack front no: 1											
	Coordinate		Elliptical parameter						da/dn (mm/kc)		
No	x	y	a	c	ϕ	ΔK $MPa\sqrt{m}$	S_{op}	$\Delta Keff$ $MPa\sqrt{m}$	test	based on ΔK	based on $\Delta Keff$
1	11.71	2.02	7.83	12.12	15	20.95	34.5	17.93	1.16	1.64	1.99
2	10.50	3.92	7.83	12.12	30	20.22	31.5	17.75	1.05	1.41	1.85
3	8.57	5.54	7.83	12.12	45	20.34	30.0	18.08	0.94	1.38	1.88
4	6.06	6.78	7.83	12.12	60	20.84	30.0	18.53	0.86	1.45	1.97
5	3.14	7.56	7.83	12.12	75	21.35	30.0	18.97	0.80	1.54	2.09
6	0.00	7.83	7.83	12.12	90	21.55	27.0	19.64	0.79	1.58	2.30

Specimen : PCA15 Crack front no: 2											
	Coordinate		Elliptical parameter						da/dn (mm/kc)		
No	x	y	a	c	ϕ	ΔK $MPa\sqrt{m}$	S_{op}	$\Delta Keff$ $MPa\sqrt{m}$	test	based on ΔK	based on $\Delta Keff$
1	10.66	1.96	7.59	11.04	15	19.97	37.5	16.74	0.91	1.27	1.43
2	9.56	3.80	7.59	11.04	30	19.16	34.5	16.40	0.84	1.13	1.37
3	7.81	5.37	7.59	11.04	45	19.16	33.0	16.60	0.78	1.13	1.42
4	5.52	6.57	7.59	11.04	60	19.54	31.5	17.15	0.73	1.20	1.56
5	2.86	7.33	7.59	11.04	75	19.96	31.5	17.52	0.70	1.27	1.66
6	0.00	7.59	7.59	11.04	90	20.13	30.0	17.82	0.69	1.30	1.77

Specimen : PCA15 Crack front no: 3											
	Coordinate		Elliptical parameter						da/dn (mm/kc)		
No	x	y	a	c	ϕ	ΔK $MPa\sqrt{m}$	S_{op}	$\Delta Keff$ $MPa\sqrt{m}$	test	based on ΔK	based on $\Delta Keff$
1	9.82	1.79	6.93	10.17	15	18.41	39.0	15.14	0.78	1.01	1.09
2	8.81	3.46	6.93	10.17	30	17.85	37.5	14.87	0.73	0.92	1.04
3	7.19	4.90	6.93	10.17	45	17.96	36.0	15.16	0.68	0.94	1.10
4	5.08	6.00	6.93	10.17	60	18.38	34.5	15.72	0.65	0.85	1.22
5	2.63	6.69	6.93	10.17	75	18.79	33.0	16.28	0.63	1.07	1.35
6	0.00	6.93	6.93	10.17	90	18.96	31.5	16.64	0.62	1.10	1.43

Specimen : PCA15 Crack front no: 4											
	Coordinate		Elliptical parameter						da/dn (mm/kc)		
No	x	y	a	c	ϕ	ΔK $MPa\sqrt{m}$	S_{op}	$\Delta Keff$ $MPa\sqrt{m}$	test	based on ΔK	based on $\Delta Keff$
1	9.12	1.63	6.30	9.44	15	18.28	37.5	14.17	0.66	0.99	0.90
2	8.18	3.15	6.30	9.44	30	18.25	36.0	14.06	0.64	0.98	0.88
3	6.68	4.45	6.30	9.44	45	18.19	34.5	14.45	0.63	0.97	0.95
4	4.72	5.46	6.30	9.44	60	18.11	34.5	14.84	0.63	0.96	1.03
5	2.44	6.08	6.30	9.44	75	17.77	31.5	15.59	0.63	0.91	1.19
6	0.00	6.30	6.30	9.44	90	17.92	30.0	15.94	0.63	0.93	1.27

Specimen : PCA15 Crack front no: 5											
	Coordinate		Elliptical parameter						da/dn (mm/kc)		
No	x	y	a	c	ϕ	ΔK $MPa\sqrt{m}$	S_{op}	$\Delta Keff$ $MPa\sqrt{m}$	test	based on ΔK	based on $\Delta Keff$
1	8.53	1.48	5.70	8.83	15	15.71	34.5	13.44	0.55	0.64	0.77
2	7.65	2.85	5.70	8.83	30	15.57	33.0	13.49	0.55	0.62	0.78
3	6.24	4.03	5.70	8.83	45	15.92	34.5	13.62	0.55	0.66	0.80
4	4.42	4.94	5.70	8.83	60	16.44	31.5	14.43	0.56	0.73	0.95
5	2.28	5.50	5.70	8.83	75	16.86	28.5	15.18	0.57	0.78	1.10
6	0.00	5.70	5.70	8.83	90	17.03	28.5	15.32	0.58	0.80	1.13

Specimen : PCA15 Crack front no: 6											
	Coordinate		Elliptical parameter						da/dn (mm/kc)		
No	x	y	a	c	ϕ	ΔK $MPa\sqrt{m}$	S_{op}	$\Delta Keff$ $MPa\sqrt{m}$	test	based on ΔK	based on $\Delta Keff$
1	8.04	1.32	5.12	8.32	15	14.49	30.0	12.88	0.46	0.50	0.68
2	7.20	2.56	5.12	8.32	30	14.55	34.5	12.45	0.49	0.51	0.62
3	5.88	3.62	5.12	8.32	45	15.03	34.5	12.86	0.53	0.56	0.68
4	4.16	4.43	5.12	8.32	60	15.60	31.5	13.69	0.56	0.62	0.82
5	2.15	4.94	5.12	8.32	75	16.05	28.5	14.44	0.59	0.68	0.95
6	0.00	5.12	5.12	8.32	90	16.21	27.0	14.77	0.60	0.70	0.96

Specimen : PCA15 Crack front no: 7											
	Coordinate		Elliptical parameter						da/dn (mm/kc)		
No	x	y	a	c	ϕ	ΔK $MPa\sqrt{m}$	S_{op}	$\Delta Keff$ $MPa\sqrt{m}$	test	based on ΔK	based on $\Delta Keff$
1	7.63	1.82	4.57	7.90	15	13.34	27.0	12.15	0.39	0.40	0.58
2	6.84	2.28	4.57	7.90	30	13.60	31.5	11.94	0.41	0.42	0.55
3	5.59	3.23	4.57	7.90	45	14.20	28.5	12.78	0.44	0.48	0.67
4	3.95	3.96	4.57	7.90	60	14.83	28.5	13.35	0.47	0.54	0.76
5	2.04	4.41	4.57	7.90	75	15.30	28.5	13.77	0.49	0.59	0.83
6	0.00	4.57	4.57	7.90	90	15.47	25.5	14.27	0.50	0.61	0.92

Specimen : PCA15 Crack front no: 8											
	Coordinate		Elliptical parameter						da/dn (mm/kc)		
No	x	y	a	c	ϕ	ΔK $MPa\sqrt{m}$	S_{op}	$\Delta Keff$ $MPa\sqrt{m}$	test	based on ΔK	based on $\Delta Keff$
1	7.31	1.05	4.07	7.57	15	12.28	24.0	11.46	0.30	0.31	0.49
2	6.56	2.04	4.07	7.57	30	12.73	27.0	11.60	0.35	0.35	0.51
3	5.35	2.88	4.07	7.57	45	13.44	25.5	12.40	0.40	0.41	0.61
4	3.78	3.52	4.07	7.57	60	14.13	25.5	13.03	0.45	0.47	0.71
5	1.96	3.93	4.07	7.57	75	14.62	24.0	13.65	0.48	0.52	0.81
6	0.00	4.07	4.07	7.57	90	14.80	24.0	13.81	0.49	0.54	0.84

Specimen : PCA15 Crack front no: 9											
	Coordinate		Elliptical parameter						da/dn (mm/kc)		
No	x	y	a	c	ϕ	ΔK $MPa\sqrt{m}$	S_{op}	$\Delta Keff$ $MPa\sqrt{m}$	test	based on ΔK	based on $\Delta Keff$
1	7.03	0.93	3.60	7.28	15	11.27	22.5	10.64	0.30	0.24	0.40
2	6.30	1.80	3.60	7.28	30	11.89	24.0	11.10	0.33	0.28	0.45
3	5.15	2.54	3.60	7.28	45	12.71	24.0	11.86	0.37	0.35	0.54
4	3.64	3.12	3.60	7.28	60	13.44	24.0	12.55	0.41	0.41	0.64
5	1.88	3.48	3.60	7.28	75	13.95	22.5	13.17	0.44	0.45	0.73
6	0.00	3.60	3.60	7.28	90	14.12	22.5	13.34	0.44	0.47	0.76

APPENDIX 2 NEWMAN-RAJU SOLUTION FOR SEMI-ELLIPTICAL SURFACE CRACKS

The stress intensity factor, K, along the crack front of semi-elliptical surface cracks in a finite plate can written as:

$$K = S\sqrt{\pi a/Q}\, F_s(a/t, a/c, c/b, \phi)$$

The factor Q can be accurately approximated by:

$$Q = 1 + 1.464(a/c)^{1.65} \quad \text{for} \quad a/c \le 1$$

$$Q = 1 + 1.464(c/a)^{1.65} \quad \text{for} \quad a/c > 1$$

The boundary-correction factors, F_S, were obtained from finite-element calculation fitted to double series polynomial of a/c and a/t. The function F_S was chosen to be

$$F_s = [M_1 + M_2(a/t)^2 + M_3(a/t)^4]\, g\, f_\phi\, f_w$$

for $a/c \le 1$

$$M_1 = 1.13 - 0.09(a/c)$$

$$M_2 = -0.54 + 0.89/[0.2 + (a/c)]$$

$$M_3 = 0.5 - [1/(0.65 + a/c)] + 14(1 - a/c)^{24}$$

$$g = 1 + [0.1 + 0.35(a/t)^2](1 - \sin\phi)^2$$

$$f_\phi = [(a/c)^2 \sin^2\phi + \cos^2\phi]^{0.25}$$

$$f_w = [\sec(\pi c/2b(\sqrt{a/t}))]^{0.5}$$

for $a/c > 1$

$$M_1 = \sqrt{c/a}(1 + 0.04c/a)$$

$$M_2 = 0.2(c/a)^4$$

$$M_3 = -0.11(c/a)^4$$

$$g = 1 + [0.1 + 0.35(c/a)(a/t)^2](1 - \sin\phi)^2$$

f_w and f_ϕ are the same for $a/c \le 1$